Single-cell-resolution transcriptome map revealed novel genes involved in testicular germ cell progression and somatic cells specification in Chinese tongue sole with sex reversal

Hong-Yan Wang[1,2,12], Xiang Liu[1,3,12], Jian-Yang Chen[4,5,8,12], Yingyi Huang[1,3], Yifang Lu[1,6], Fujian Tan[4,5], Qun Liu[4,5], Mingming Yang[4,5], Shuo Li[1,6], Xianghui Zhang[1,7], Yating Qin[4,5,8], Wenxiu Ma[1,9], Yingming Yang[1,2], Liang Meng[4,5,8], Kaiqiang Liu[1,2], Qian Wang[1,2], Guangyi Fan[4,5], Rafael H. Nóbrega[10], Shanshan Liu[4,5,8]*, Francesc Piferrer[11]*, Changwei Shao[1,2] *

[1]Key Lab of Sustainable Development of Marine Fisheries, Ministry of Agriculture and Rural Affairs, Yellow Sea Fisheries Research Institute, Chinese Academy of Fishery Sciences, Qingdao 266072, Shandong, China

[2]Laboratory for Marine Fisheries Science and Food Production Processes, Qingdao National Laboratory for Marine Science and Technology, Qingdao 266071, China

[3]College of Fisheries and Life Science, Shanghai Ocean University, Shanghai 201306, China

[4]BGI Research-Qingdao, BGI, Qingdao, 266555, China

[5]BGI-Shenzhen, Shenzhen 518083, China

[6]School of Marine Sciences, Ningbo University, Ningbo 315211, Zhejiang, China

[7]College of Marine Technology and Environment, Dalian Ocean University, Dalian 116023, Liaoning, China

[8]Qingdao-Europe Advanced Institute for Life Sciences, BGI-Shenzhen, Qingdao 266555, China

[9]College of Life Sciences, Shandong Normal University, Jinan 250014, Shandong, China

[10]Reproductive and Molecular Biology Group, Department of Structural and Functional Biology, Institute of Biosciences, São Paulo State University (UNESP), Botucatu, São Paulo, Brazil

[11]Institut de Ciències del Mar (ICM), Spanish National Research Council (CSIC), Barcelona, Spain

[12]These authors contributed equally

*Correspondence: shaocw@ysfri.ac.cn (C.S.), piferrer@icm.csic.es (F.P.), liushanshan@genomics.cn (S.L.)

Abstract

Female-to-male sex reversals (pseudomales) are common in lower vertebrates and have been found in natural populations, which is a concern under rapid changes in environmental conditions. Pseudomales can exhibit altered spermatogenesis. However, the regulatory mechanisms underlying pseudomale spermatogenesis remain unclear. Here, we characterized spermatogenesis in Chinese tongue sole (*Cynoglossus semilaevis*), a species with genetic and environmental sex determination, based on a high-resolution single-cell RNA-seq atlas of cells derived from the testes of genotypic males and pseudomales. We identified five germ cell types and six somatic cell types and obtained a single-cell atlas of dynamic changes in gene expression during spermatogenesis in Chinese tongue sole, including alterations in pseudomales. We detected decreased levels of Ca^{2+} signaling pathway-related genes in spermatogonia, insufficient meiotic initiation in spermatocytes, and a malfunction of somatic niche cells in pseudomales. However, a cluster of *CaSR* genes and MAPK signaling factors were upregulated in undifferentiated spermatogonia of pseudomales. Additionally, we revealed that Z chromosome-specific genes, such as *piwil2*, *dhx37,* and *ehmt1*, were important for spermatogenesis. These results improve our understanding of reproduction after female-to-male sex-reversal and provide new insights into the adaptability of reproductive strategies in lower vertebrates.

Key words: *Cynoglossus semilaevis*, spermatogenesis, single-cell transcriptome, sex reversal, spermatogonia

Introduction

Vertebrate spermatogenesis is a highly conserved process by which diploid spermatogonial stem cells (SSCs) undergo self-renewal and differentiation, meiosis, and ultimately produce haploid spermatozoa carrying a recombined genome (Hess and Renato de Franca, 2008; Schulz et al., 2010). SSCs as the starting point of germline cells, must balance self-renewal and differentiation for the constant generation of mature gametes. This process relies on interplay between testicular niche cells and germ cells. Luteinizing hormone (LH) stimulates the secretion of steroid hormones by Leydig cells and the production of growth factors by Leydig and Sertoli cells, which, in combination, regulate the proliferation and differentiation of spermatogonia (Schulz et al., 2005). Glial cell line-derived neurotrophic factor (GDNF), a secretion in Sertoli cells, is thought to facilitate SSC proliferation via multiple signaling pathways, such as the PI3K/AKT signaling pathway, Src family kinase signaling pathway, and Ras/ERK signaling pathway (He et al., 2008; Lee et al., 2007; Oatley et al., 2007). Retinoic acid (RA) secreted by Sertoli cells promotes spermatogonial differentiation with the activation of transcription regulator *MAFB* (Raverdeau et al., 2012). The initiation of meiosis precedes the replication of chromosomal DNA and is dependent on the activation of RA/Stra8 signaling (Baltus et al., 2006; Endo et al., 2015). Spermatogonia undergo DNA replication, chromosomal synapsis, DNA double-strand breaks, DNA recombination, separation of chromosomes, and finally the formation of two secondary spermatocytes. After the second meiotic division, round spermatids are formed, in turn forming mature sperm following complex morphological changes. Recently, single-cell RNA-seq has been

used to construct maps of the molecular signature of spermatogenesis in vertebrates, such as human, mouse, monkeys, and chicken (Estermann et al., 2020; Green et al., 2018; Guo et al., 2018; Lau et al., 2020a; Wang et al., 2018), providing an in-depth understanding and comprehensive biological insights into vertebrate reproduction.

Discrepancies between genetic and physiological or gonadal sex are sometimes encountered across vertebrates. The etiology varies, including genetic and environmental causes, depending on the vertebrate taxa. A discrepancy between gonadal and genetic sex is referred to as a sex reversal. Female-to-male sex reversals are called pseudomales or neomales. Sex reversals have been documented in all vertebrate classes, from fish to mammals (Piferrer and Anastasiadi, 2021). For example, in humans, 46^{XX} male syndrome, characterized by infertility, involves the loss of the entire Y chromosome, and the deletion of the azoospermia factor (AZF) region of the Y chromosome causes defects in spermatogenesis (Chiang et al., 2013). Notably, reports of environmental sex reversal are increasing in lower vertebrates, such as reptiles (Stelkens and Wedekind, 2010), amphibians (Quinn et al., 2007), and fish (Li et al., 2022; Narita et al., 2007; Piferrer and Anastasiadi, 2021; Valdivieso et al., 2022; Xiong et al., 2020). Although the proportion of spermatocytes was significantly reduced in XX testis, both XY-normal male and XX-pseudomale medaka undergo functional spermatogenesis (Myla et al., 2021). In addition, despite differences in the clustering and development of Leydig cells, similarities in the morphological structure of the testis, distribution of Sertoli cells, and development of germ cells were observed in primary males and female-to-male sex-reversals in rusty parrotfish (Abdel-Aziz et al., 2012). Recently, a reduced number of spermatozoa has been observed in the testis of neomale zebrafish (Valdivieso et al., 2022). Thus, in

addition to interspecific differences, the mechanism underlying the generation of fertile spermatids in female-to-male sex-reversals of lower vertebrates is not well understood. This is of relevance for conservation biology because neomales have been discovered in natural populations of fishes and reptiles (Valdivieso et al., 2022).

Chinese tongue sole (*Cynoglossus semilaevis*) is a benthic flatfish with a clear sexual dimorphism and female heterogametic sex determination system (ZZ♂/ZW♀). In the sensitive developmental period, high temperatures can induce the sex reversal of female fish (ZW♀) to pseudomales (ZW♂) (Chen et al., 2014). Notably, pseudomales resemble normal males phenotypically since they can develop mature gonads and produce fertile Z-gametes, although W-gametes have not been found (Chen et al., 2014). Thus, Chinese tongue sole can be used as a suitable model to investigate the mechanism underlying fertility in species with sex reversal.

Here, we analyzed the heterogeneity of testicular cells and revealed the dynamic gene expression changes during spermatogenesis in Chinese tongue sole at single-cell resolution. By a comparative analysis of spermatogenesis between males and pseudomales, phenotypic and gene expression differences during spermatogenesis in populations with sex reversal were explored. Our data provide a reference for further studies of fish reproductive biology and support research on the conservation and diversity of spermatogenesis in vertebrates at different evolutionary scales. More significantly, we systematically characterized a series of biological processes from spermatogonia self-renewal and differentiation to spermatogenesis in pseudomales. These observations provide novel insights into the mechanism of spermatogenesis in pseudomales and the adaptability of reproductive strategies in lower vertebrates.

Results

Global transcriptional profiling of Chinese tongue sole testicular cells

Using the iDrop system, the testes of male and pseudomale Chinese tongue sole were evaluated by a single-cell transcriptional analysis **(Figure 1A)**. After sex reversal, the gonads of Chinese tongue sole showed substantial morphological similarity to the testes of regular male fish **(Figure 1B)**. We created 11 libraries for males and 7 libraries for pseudomales. After quality control, we obtained the transcriptional spectra for 31739 cells. To minimize batch effects from sample processing, we integrated all 18 scRNA-seq datasets using the mutual nearest neighbor (MNN) methodology. On average, each cell had 6050 unique molecular identifiers (UMIs) and 2606 genes. After data integration, the transcriptional profiles were assigned to 16 cell clusters by uniform manifold approximation and projection (UMAP) analyses **(Figure S1A)**. There was no obvious difference in cell distribution between males and pseudomales **(Figure S1B)**. All clusters were included in each sample **(Figure S1C)**.

We annotated cell identities based on marker expression and differentially expressed genes (DEGs). We performed differential expression analyses across groups. Based on gene expression patterns, we assigned the 11 known cell types to five germ cell populations as well as six somatic cell populations **(Figure 1C and D)**. According to a functional enrichment analysis, DEGs in undifferentiated spermatogonia (Undiff SPG) were enriched in “purine nucleotide biosynthetic process”, “spermatogenesis”, and “cellular macromolecule catabolic process”, DEGs in differentiated spermatogonia (Diff.ed SPG) were enriched for the terms “RNA processing” and “pre-replicative complex assembly”, DEGs in preleptotene spermatocytes (pre-Lep) and pachytene spermatocytes (P-SPC) were enriched for the

terms “DNA replication” and “M phase”, and DEGs in sperm were enriched in “cilium or flagellum-dependent cell motility” and “modification-dependent protein catabolic process” **(Figure 1E)**. By contrast, Sertoli cell DEGs were enriched in “tight junction” and “cell adhesion”, while Leydig cells were enriched for the terms “response to hormone” and “steroid metabolic process.” In addition, the terms “innate immune system”, “T cell receptor signaling pathway”, “adaptive immune system”, and “transport of small molecules” were enriched for NKT cells, T cells, B cells, and erythrocytes, respectively **(Figure S2A)**.

We identified a number of marker genes reported to be specifically expressed in various cell types of the testis in zebrafish and mammals. We classified germ cell types as follows: spermatogonia (*gfrα1*, *zbtb16*, *dnd1*, *stmn1*, etc.) (Guillaume et al., 2010; Guo et al., 2017; Law et al., 2019; Yamaji et al., 2017), spermatocytes (*sycp3*, *ccne2*, *ccnb1*, *e2f2, spo11*, etc.) (Lau et al., 2020b; Lauper et al., 1998; Wang et al., 2018), and spermatid/spermatozoa (*cfap69*, *dnah3*, d*najb13, tekt1*, etc.) (Guan et al., 2009; Ming et al., 2001; Neesen et al., 1997; Wang et al., 2020) **(Figure 1F and Figure S2B)**. Some spermatogonial genetic markers were expressed in both Undiff SPG and Diff.ed SPG. We analyzed the expression of additional spermatogonial markers in these cells and found that Undiff SPG expressed more genes involved in the maintenance of stemness and began to express genes related to spermatogonial differentiation in Diff.ed SPG **(Figure S2C)**.

In addition to germ cells, we also analyzed somatic cells in the gonads and identified six somatic cell types. These cells were annotated based on DEGs and reported genetic markers. Somatic cells were identified as Sertoli cells (*inha*, *gata4*, etc.) (Zhao et al., 2020) and Leydig cells (*cyp11a1*, *cyp11b2*, etc.) (Lau et al., 2020b).

We also identified other somatic cells, such as NKT cells (*cxcr4*, *impa1*, etc.) (Young et al., 2018), B cells (*swap70* and *irf8*) (Young et al., 2018), T cells (*cd2l* and *cd247*) (Hurley et al., 1994; Lundholm et al., 2010), and erythrocytes (*hbad*, *hba1* and *gp9l*) (Munday et al., 2000; Tsang et al., 2017) **(Figure 1F and Figure S2B)**.

Next, fluorescence *in situ* hybridization (FISH) was performed to validate the expression patterns of *gfrα1*, *ccnb1*, *ccne2*, *gata4*, *inha,* and *cyp11a1.* We found that *gfrα1*, *ccnb1*, and *ccne2* were actively transcribed in germ cells located in the seminal vesicle, while *gata4*, *inha*, and *cyp11a1* were expressed in the space between seminal vesicles **(Figure 1G and Figure S2D)**. Notably, *ccnb1* showed a similar expression pattern in each cell in one spermatogenic vesicle, indicating that they are in the same cell cycle phase. This suggested that all germ cells in a spermatogenic vesicle might be in the same state in the cell cycle. Additionally, we confirmed specific expression of *mcama*, *cks2*, *marcksl1b,* and *pydn*, the top DEGs in Undiff SPG, P-SPC, Sertoli cells, and Leydig cells, respectively **(Figure S2E)**. These genes provide new resources as candidate marker genes for each cell type.

We identified the same cell types in Chinese tongue sole testis as those in humans and mice. To examine the conservation of the process of spermatogenesis between teleosts and mammals, we obtained genetic markers of different testis cells from published single-cell atlases of the human and mouse testes with high accuracy (Green et al., 2018; Wang et al., 2018). The expression patterns of these genes in human, mouse, and Chinese tongue sole testis cells were highly similar, such as *gfra1*, *spo11*, *sycp1, sycp3, dnajb13, tekt1,* and *gata4* **(Figure 1H)**. These results suggested that during evolution, the process of male gamete production was conserved for the maintenance of reproduction across species. However, expression levels of some

genes (e.g., *hsd11b2*, *zbtb16,* and *id4*) were similar in mouse and Chinese tongue sole but different from those in human **(Figure 1H)**. Therefore, the process is generally well conserved; however, substantial differences within a given group of vertebrates (human vs. mouse), rather than across vertebrate taxa, are possible.

Dynamic patterns of gene expression during spermatogenesis in Chinese tongue sole

Using Monocle2, we reconstructed a trajectory of gene expression changes during spermatogenesis. Using the trajectory from spermatogonia to spermatozoa **(Figure 2A; Figure S3A and S3B)**, we analyzed the expression patterns of genes by an unsupervised pseudotime analysis during spermatogenesis, revealing four distinct gene cohorts **(Figure 2B)**. Interestingly, more genes were expressed in early spermatogenesis (spermatogonia) than in differentiated cell stages. This may be attributed to the fact that spermatogonia are the foundation from which males continually produce millions of genetically unique gametes (Law et al., 2019). Considering the expression trends in germ cell marker genes in our single-cell RNA data, we found that levels of *dnd1* and *id4*, which were associated with the self-renewal of spermatogonia, decreased gradually during spermatogenesis. Cell proliferation-related transcription factors *e2f2* and DNA polymerase *pole* were most highly expressed in the spermatocyte phase. *Tekt1* and *dnajb13,* which were related to sperm flagellum structure and sperm motility, were highly expressed at the end of spermatogenesis **(Figure 2C)**.

To obtain a detailed view of the sperm maturation process, we re-clustered the

spermatid/spermatozoa cells and uncovered four transcriptionally distinct clusters (S1–S4) representing the four stages of sperm differentiation: initial spermatids, intermediate spermatids, final spermatids, and spermatozoa(Leal et al., 2009) **(Figure 2D)**. Male and pseudomale samples were evenly distributed in each cluster, indicating that there were no pseudomale-specific sperm subsets **(Figure S3C)**. We detected the DEGs in each cluster and genes with highly variable expression. There were obvious differences in gene expression among subclusters **(Figure 2E)**. The round spermatid marker *stard10* (Culty et al., 2015) and spermatocyte marker *hells* were highly expressed in S1, while the cell division inhibitory factor *cdkn3* (Culty et al., 2015) and histone 4 (*h4*) (Kurtz et al., 2007) were specifically expressed in S2. Additionally, the sperm autoantigenic gene *spag17* (Kazarian et al., 2018) and the cilia and flagella-associated gene *cfap69* were specifically expressed in S3 and S4, respectively **(Figure 2F)**. A functional enrichment analysis of DEGs revealed that the term "regulation of cell cycle" was highly enriched in S1, indicating that S1 represented the phase immediately after meiosis. S2 was enriched for the terms of "protein catabolic process", while S3 and S4 specifically express flagella-related genes, indicating that these cells are final spermatids and spermatozoa **(Figure S3D)**. Moreover, Monocle3 was used to analyze the process of spermiogenesis. Outcomes of a trajectory analysis showed the correct ordering of mature sperm in pseudotime **(Figure 2G)**. Furthermore, we analyzed the dynamic expression patterns of genes during spermiogenesis and found some functionally related genes (e.g., *mycb*, *hsp90ab1*, *wipi1*, and *cfap20*) expressed in different groups **(Figure S3E)**. In summary, our results provided a dynamically regulated transcriptome during fish spermatogenesis in a perfectly orchestrated stage-specific manner.

Integrated comparison of dynamic gene expression during spermatogenesis between males and pseudomales

Testes from pseudomale (ZWm) and male (ZZm) Chinese tongue sole showed similar histological characteristics and structures (**Figure 1B**). When we integrated single-cell libraries, we found that the pseudomale and male testicular cells were evenly distributed in the UMAP **(Figure S1B)**. This indicated that pseudomales and males had the same testicular cell types. Furthermore, the pseudomales and males showed similar gene expression patterns **(Figure S4A)**. In summary, spermatogenesis and gene expression patterns were highly similar in genetic males and pseudomales.

However, pseudomale fish are the product of sex reversal, i.e., a genetic female that instead of developing ovaries develops testis during sexual differentiation. We hypothesized that because of its origins, specific genetic regulatory mechanisms affect the process of spermatogenesis in pseudomale fish. First, in the analysis of relative cell frequencies, pseudomale fish had a higher proportion of Undiff SPG and lower relative frequencies of Diff.ed SPG and pre-Lep ($p < 0.05$) than those of regular males **(Figure 3A)**. Furthermore, we counted the primary spermatocytes of testes derived from five males and pseudomales **(Figure S4B and S4C)**. The primary spermatocytes in pseudomales were significantly lower than corresponding counts in males ($p < 0.05$) **(Figure S4D)**. These data suggested that the difference between pseudomales and males can be attributed to a difference in the number of spermatogonia that differentiate and progress to spermatocytes and hence the higher number of Undiff SPG observed in pseudomales. We further analyzed the differences in genes expressed in different cell types between males and pseudomales. In total, we

observed 3629 DEGs between males and pseudomales. Genes up-regulated in pseudomales ($p < 0.05$, Log2FC > 2) were enriched for the terms “response to endogenous stimulus” and “negative regulation of cell differentiation”. Up-regulated genes in males ($p < 0.05$, Log2FC > 2) were enriched for terms such as “calcium signaling pathway” and “steroid biosynthetic process” **(Figure 3B)**. In view of the substantial difference in the proportion of Diff.ed SPG and pre-Lep, we analyzed the DEGs ($p < 0.05$, |Log2FC| > 1) of these two germ cells in males and pseudomales **(Figure S4E and S4F)**. There were 1028 and 1090 DEGs in the Diff.ed SPG and pre-Lep, respectively, between males and pseudomales. Up-regulated genes in pseudomale Diff.ed SPG were enriched in “cell-cell signaling” and “calcium ion transport” and down-regulated genes were enriched for the term “hormone metabolic process” **(Figure S4G)**. Notably, similar functional enrichment results were obtained in pre-Lep **(Figure S4H)**. Cell cycle-related genes were differentially expressed in diverse cell types. Diff.ed SPG and pre-Lep expressed some G1/S-related genes, and the expression levels were higher in males than in pseudomales. However, there were no obvious differences in G2/M-related gene expression between males and pseudomales **(Figure 3C)**.

The initiation of spermatogonial differentiation in mammals has been comprehensively evaluated; however, little is known about this process in many other species. Here, we note that the expression of genes involved in cell cycle activation (*cdc45* and *meioc*) (Abby et al., 2016; Lin et al., 2008; Wu and Nurse, 2014) differed between males and pseudomales **(Figure 3D)**, indicating a defect in meiosis in pseudomales.

Moreover, the autophagosome formation-related gene *ykt6* (Bas et al., 2018) and

297 facilitator of apoptosis *znrf3* (Colozza and Koo, 2021) were significantly up-regulated
298 in Diff.ed SPG and pre-Lep of pseudomales ($p < 0.05$) **(Figure 3E)**. Our results
299 showed that the initiation of spermatocyte meiosis in pseudomale fish is possibly
300 inhibited and accompanied by autophagy.

301

302 **Undifferentiated spermatogonia of pseudomales showed obvious transcript**
303 **heterogeneity**

304 Spermatogonia are the starting point of spermatogenesis, and their self-renewal and
305 differentiation are strictly regulated to maintain germ cells. In total, 1373 DEGs in
306 Undiff SPG between pseudomales (ZWm) and males (ZZm) are shown in **Figure 4A**.
307 Up-regulated genes in the pseudomale Undiff SPG were particularly enriched for the
308 terms "cell-cell signaling", "cell proliferation", and "MAPK family signaling
309 cascades", whereas down-regulated genes were enriched for the terms "calcium
310 signaling pathway" and "metabolism of steroids" **(Figure 4B)**.

311 Genes in the MAPK pathway, involved in many male reproductive processes,
312 including spermatogenesis, sperm maturation and activation, capacitation, and the
313 acrosome response (Li et al., 2009), showed expression differences between
314 pseudomales and males. For example, expression levels of *pla2g4a*, *gdpd1,* and
315 *morn3*, which are related to the testis physiology and spermatogenesis (Fujihara et al.,
316 2019; Kurusu et al., 2011; Zhang et al., 2015), were higher in Undiff SPG of
317 pseudomales than in males **(Figure 4C)**.

318 We also found that calcium sensing receptor (*CaSR*), an activator of different
319 MAPK pathways (McGowan et al., 2002), was overexpressed in the testis of

pseudomales **(Figure 4D)**. *CaSR* is a member of the G protein-coupled receptors and is widely distributed; it maintains the homeostasis of metal ions in the body, regulates hormone secretion, and activates ion channels (Conigrave and Ward, 2013). Interestingly, we found 27 copies of *CaSR* in the Chinese tongue sole genome, compared with only one copy in the human genome, indicating gene expansion. The genes are tandemly arranged, and 21 out of 27 *CaSR* copies were more highly expressed in Undiff SPG of pseudomales than males ($p < 0.05$) **(Figure 4D)**.

However, genes in the Ca^{2+} signaling pathway were down-regulated in pseudomale Undiff SPG **(Figure 4E)**, indicating that this pathway may be suppressed in pseudomale Undiff SPG. Genes in the Ca^{2+} signaling pathway are related to spermatogenesis and germ cell development in mammals; for example, *vdac3*, *ryr3,* and *gnaq* were decreased in pseudomale Undiff SPG. Voltage-dependent anion channel (*VDAC*) exists in mammalian spermatozoa and is involved in spermatogenesis and sperm functions (Pan et al., 2017). Ryanodine receptors (*RyRs*) are intracellular calcium release channels, which are expressed in germ cells and cooperate with calcium channels for the regulation of male maturation (Chiarella et al., 2004). Our results suggested that the Ca^{2+} signaling pathway was impaired in pseudomale Undiff SPG. By contrast, *CaSR* and the downstream MAPK signaling pathway were activated to maintain spermatogenesis.

Gdnf, maintaining the stemness of SSC, was generally expressed in spermatogonia. Notably, *gfrα1* and *ret*, the complex receptors for *gdnf* located in the SSC membrane, were highly expressed in pseudomale Undiff SPG **(Figure 4F)**. This indicated that Undiff SPG of pseudomales have stronger self-renewal activity, which might explain the elevation in Undiff SPG in pseudomales.

Gene expression pattern on sex chromosomes

Although pseudomales can produce mature sperms, no sperm containing the W chromosome has been detected (Chen et al., 2014). Many Z-specific genes are involved in spermatogenesis. The deficiency in spermatogenesis-related genes on the W chromosome likely explains the loss of W sperm (Meng et al., 2014). We analyzed the expression patterns of genes specific to the Z chromosome and detected higher expression levels in male fish than in pseudomale fish **(Figure 5A, top)**. However, only a few autosomal genes are differentially regulated between males and pseudomales **(Figure 5A, bottom)**. A functional enrichment analysis of Z-specific genes revealed that these genes were enriched for various signaling pathways, such as "RNA processing", "translation synthesis", "chromosome organization", and "positive regulation of cell cycle process" **(Figure 5A, right)**. These processes are all closely related to spermatogenesis (Agarwal et al., 2021; Griswold, 2016; Watanabe and Lin, 2014).

The dysregulation of piRNAs regulating key proteins involved in spermatogenesis has been found in idiopathic non-obstructive azoospermia (Cao et al., 2018; Kamaliyan et al., 2018). We found that piRNA-related proteins were differentially regulated between male and pseudomale fish among Z-specific genes. We analyzed the expression of Z-specific genes related to piRNAs and found that those genes are generally expressed at lower levels in pseudomales than males **(Figure 5B)**. *Piwil2* (piwi-like RNA-mediated gene silencing 2), which is essential for germline integrity during spermatogenesis by repressing transposable elements (De Fazio et al., 2011), was expressed at lower levels during spermatogenesis in pseudomales than in males.

Another piRNA-related gene, *dgcr8*, a subunit of the microprocessor complex that mediates the biogenesis of microRNAs from the primary microRNA transcript (Wang et al., 2007), showed lower levels of expression in pseudomales than in males. In addition, we found that some other Z-specific genes were differentially expressed between males and pseudomales. Pathogenic variants in the DEAH-box RNA helicase *DHX37* are a frequent cause of 46^{XY} testicular regression syndrome (McElreavey et al., 2020). Our data indicated that *dhx37* is down-regulated in pseudomales. Furthermore, we found that genes encoding cell cycle proteins, such as *anapc7* and *psmd9,* which are associated with spermatogenesis, as well as the histone modification enzyme *ehmt1* were down-regulated in pseudomales **(Figure 5C)**.

Although the expression of Z-specific genes was higher in males than pseudomales, we did not consistently observe two-fold higher expression in males than in pseudomales. Local dosage compensation on the Z chromosome has been reported in pseudomale testes (Shao et al., 2014). Of note, many of the genes described above were located in this region. We further tested the expression levels of genes in this region in different cell types and found that the average expression of the entire Z chromosome in pseudomale fish was half that of male fish **(Figure 5D)** and expression levels were up-regulated in the dosage compensation region **(Figure 5E)**.

Pseudomale niche cells exhibited abnormal gene expression patterns

Sertoli cells and Leydig cells play a supporting role in spermatogenesis. Interestingly, the proportion of pseudomale Leydig cells was lower ($p < 0.05$) than that of males **(Figure 6A)**. To explore the heterogeneity of the spermatogenesis environment in

391 pseudomale fish, we first evaluated differences in gene expression in Leydig cells
392 between pseudomales and males. We found 352 up-regulated and 75 down-regulated
393 genes in pseudomales **(Figure 6B)**. Various terms, such as "steroid metabolic
394 process", "response to hormone", and "drug metabolic process", were enriched in
395 down-regulated genes of pseudomale Leydig cells. "Cellular response to DNA
396 damage stimulus" and "ncRNA metabolic process" were enriched in up-regulated
397 genes **(Figure 6C)**. Notably, we found that *hsd3b1*, *cyp17a1*, *cyp11a1*, *hsd11b2*, and
398 *hsd17b1,* among other genes with key roles in the synthesis of testosterone, were
399 highly expressed in Leydig cells in males and significantly down-regulated in
400 pseudomales. Furthermore, the expression levels of *fshr* and *lhcgr*, the receptors of
401 follicle-stimulating hormone and luteinizing hormone (LH), were down-regulated in
402 pseudomales **(Figure 6D)**. Together, these results suggested that Leydig cells of
403 pseudomales showed lower *lhcgr* expression and had difficulty responding to LH
404 stimulation, resulting in abnormal development and testosterone production.

405 Subsequently, we evaluated differences in gene expression in Sertoli cells. In total,
406 344 and 326 DEGs were down- and up-regulated in pseudomale Sertoli cells,
407 respectively **(Figure 6E)**. Down-regulated genes in pseudomale Sertoli cells were
408 enriched for various biological processes and pathways, such as "cell adhesion" and
409 "Wnt signaling pathway." Up-regulated genes were enriched in the terms such as
410 "negative regulation of cell communication" and "supramolecular fiber organization"
411 **(Figure 6F)**. In addition, the Wnt signaling pathway inhibitors *sfrp1* and *sfrp2* (Warr
412 et al., 2009), DNA demethylation regulatory gene *tet3*, and cell structure-related
413 genes *actg1* and integrin *itga6* were expressed at lower levels in pseudomale Sertoli
414 cells **(Figure 6G)**. In general, we speculated that there might be a functionally

significant down-regulation of genes in pseudomale Sertoli cells.

To gain insight into the mechanism underlying sex determination and sex reversal in Chinese tongue sole, we investigated the expression patterns of sex determination-related genes in the testicular cells of males and pseudomales with scRNA-seq transcriptome data. Male sex-related genes were mainly expressed in Sertoli cells of males and pseudomales. Female sex-related genes were mainly located in Undiff SPG of pseudomale testes **(Figure 6H)**. These results indicated that female sex-related genes in Undiff SPG of pseudomales may reflect the classification of these animals as genotypic females.

Discussion

We obtained a high-resolution testicular cell atlas by scRNA-seq for both male and pseudomale Chinese tongue sole. Studies of the discrepancy between genetic sex and physiological sex are of relevance not only because pseudomales are increasingly found in different species of vertebrates in natural populations but also because understanding the molecular basis of spermatogenesis in pseudomales can provide useful insights into the regulation of spermatogenesis and can even contribute to the study of disorders of sexual development (DSD). Thus, a comprehensive understanding of conventional and unconventional spermatogenesis is vital for the diagnosis and management of infertility. Our single-cell transcriptomic atlas laid a solid foundation for the further investigation of spermatogenesis in individuals with sex reversal.

The conservation of spermatogenesis among mammalian species has been reported

438 (Lau et al., 2020b). Here, using the Chinese tongue sole as a model, we identified
439 undifferentiated spermatogonia, differentiated spermatogonia, preleptotene
440 spermatocytes, pachytene-spermatocytes, and spermatid/spermatozoa using typical
441 markers, such as *gfra1*, *ccne2*, *ccnb1*, *sycp3,* and *dnajb13*. Other somatic cells, such
442 as Sertoli cells and Leydig cells, were identified based on *gata4* and *cyp11a1*. These
443 results indicate that signature genes of distinct cell types established in mammals
444 could serve as markers of non-mammalian poikilothermic vertebrates. Thus, the cell
445 types present in fish testes were similar to those found in mammals (Lau et al., 2020b).
446 Furthermore, the typical marker genes of spermatogenesis in mammals, such as
447 *GFRA1*, *SYCP1*, *SYCP3*, *DNAJB13*, and *TEKT1*, showed similar expression trends in
448 Chinese tongue sole. Notably, in an unsupervised pseudotime analysis, spermatogonia,
449 spermatocyte, and sperm followed a continuous trajectory. This process of
450 spermatogonia, followed by spermatocytes and sperm is consistent with the process in
451 mammals (Wang et al., 2018). These results indicate that the essential features of
452 spermatogenesis are highly conserved across vertebrate taxa.

453 Comprehensive comparative analysis of the testes from genetic males (ZZm) and
454 female-to-male sex reversed pseudomales (ZWm) provided insights into the
455 differential regulation of spermatogenesis; in addition to assessing the underlying
456 molecular endocrinology of pseudomales, the results have implications for
457 determining their reliability as a proxy for the study of certain DSDs. The pseudomale
458 fish had the same distribution of testicular cell types and highly similar DEGs to those
459 in male fish. More importantly, the cellular changes and the expression of key factors
460 during spermatogenesis were also highly similar. Together with the DNA methylation
461 patterns in pseudomales (Shao et al., 2014), our results demonstrated that various

462 characteristics (including epigenetic modification, gene expression, and cellular
463 differentiation) are similar between males and pseudomales. Despite this high degree
464 of similarity, we detected differences between the male and pseudomale testis.
465 Insufficient levels of cell cycle-related genes resulted in a lower proportion of
466 spermatocytes in pseudomales. Previous studies have revealed the key function of cell
467 cycle checkpoints during meiosis (Bolcun-Filas et al., 2014; Spruck et al., 2003;
468 Zhang et al., 2021). Our results showed that the low expression of *meioc* may cause a
469 delay in the initiation of meiosis in pseudomales **(Figure 7)**.

470 The Ca^{2+} concentration contributes to sex determination in the red-eared slider
471 (Weber et al., 2020). Georges and colleagues proposed that cellular calcium and redox
472 (CaRe) regulation function as a 'cellular sensor' of environmental conditions; the
473 signals are transduced to diverse signal transduction pathways or influence epigenetic
474 processes, ultimately driving the differential expression of sex genes (Castelli et al.,
475 2020). We also detected the downregulation of the Ca^{2+} signaling pathway and
476 upregulation of extracellular calcium sensing receptors (*CaSR*) in Undiff SPG of
477 pseudomale. The MAPK signaling may be complementary to Ca^{2+} signaling.
478 Furthermore, *CaSR* expanded in Chinese tongue sole and was highly expressed in
479 pseudomales **(Figure 7)**. Taken together, these results suggest that the regulation of
480 Ca^{2+} may be a general mechanism involved in temperature-mediated sex
481 determination and support the CaRe hypothesis (Castelli et al., 2020). However, we
482 did not establish the detailed mechanism underlying the regulation of the Ca^{2+}
483 concentration by *CaSR*. Thus, further research is needed to resolve the effects of
484 temperature on *CaSR* and the MAPK signaling pathway.

485 We analyzed the functions of genes on the Z chromosome of Chinese tongue sole in

spermatogenesis. Many genes related to spermatogenesis were located on the Z chromosome, including genes encoding piRNA-related proteins (*piwil2*, *dgcr8*, and *dhx37*), chromosome organization-related gene (*ehmt1*), and cell cycle-related genes (*anapc7* and *psmd9*). Importantly, the expression levels of these genes change dynamically during spermatogenesis. Analogously, the human Y chromosome harbors a number of genes essential for spermatogenesis, especially in the AZF region (Krausz and Casamonti, 2017). However, as most of the Y chromosome, including the AZF region, is lacking, 46^{XX} men are infertile (Chiang et al., 2013). Therefore, we suggest that the W chromosome lacks spermatogenesis-related genes, resulting in W sperm deletion in pseudomales **(Figure 7)**. This provides a perfect research model for studying infertility caused by chromosome abnormalities. Besides, although pseudomales only have a single Z chromosome, local dosage compensation plays an important role in regulating gene expression (Shao et al., 2014). This mechanism is different from the transcriptional inactivation of one X chromosome in female of mammals (Avner and Heard, 2001). In addition, we did not detect obvious meiotic sex chromosome inactivation (MSCI), suggesting that homologous recombination of Z and W chromosomes in pseudomales is still possible. This is consistent with previous studies in chickens (Guioli et al., 2012). However, the precise period of the W sperm deficiency in spermatogenesis of pseudomales is still unclear.

Leydig cells mainly synthesize and secrete steroid hormones with testosterone and 11-ketotestosterone as the main steroids, promoting spermatogenesis and maturation (Zirkin and Papadopoulos, 2018). In our study, a small proportion of pseudomale Leydig cells showed low levels of *lhcgr*. Additionally, *hsd11b2, cyp11a1, hsd17b1, cyp17a1,* and *hsd3b1*, which catalyze the conversion of cholesterol to testosterone,

were significantly down-regulated in pseudomale Leydig cells. Notably, in the human testis, mutations or deletions of *LHCGR* result in abnormal Leydig cell differentiation, with a significant decrease in number, impairment of steroid hormone synthesis, and elevated *LH*; however, there is no testosterone surge on *LH* and *hCG* stimulation, leading to male pseudohermaphroditism (Segaloff, 2009). Therefore, we suggested that a mechanism similar to human "Leydig cell agenesis" operates in the Leydig cells of Chinese tongue sole pseudomale **(Figure 7)**. The mechanism underlying the *lhcgr* reduction in pseudomales needs to be further studied. Interestingly, we detected *fshr* expression in both Leydig and Sertoli cells in Chinese tongue sole, which is expressed only in Sertoli cells in mammals. Similar observations have been reported in eel and African catfish (García-López et al., 2009; Ohta et al., 2007).

Sertoli cells are the only somatic cells that come into direct contact with germ cells, and their continuous and tight interactions with germ cells underlie spermatogenesis (Griswold, 2016). In this study, we found that genes involved in intercellular junctions as well as various signal transduction pathways were significantly down-regulated in Sertoli cells of the pseudomales, suggesting an altered interaction between Sertoli cells and germ cells in pseudomales. Furthermore, our data showed that the Wnt signaling pathway inhibitors *sfrp1* and *sfrp2* (Warr et al., 2009) were significantly down-regulated in Sertoli cells of pseudomales. Interestingly, disruptions of the Wnt signaling pathway often cause abnormal sperm morphology and function in mammals, resulting in male infertility (Qiu et al., 2016). Additionally, the abnormal activation of the Wnt signaling pathway was found in azoospermic male Sertoli cells (Zhao et al., 2020). Therefore, we speculate that the Wnt signaling pathway exhibits abnormal activation in pseudomale spermatogenesis **(Figure 7)**.

In summary, this study provides a comprehensive transcriptomic atlas of fish testes and reveals dynamic changes in gene expression patterns during spermatogenesis at single-cell resolution. The identification of 11 different cell types and their specific markers indicates the conservation of the essential features of spermatogenesis with corresponding features in mammals. Furthermore, by comparing males and pseudomales, we gained insight into the subtle but important differences of the individuals after sex-reversal. Dysregulation of Sertoli and Leydig cell function and, in particular, decreased expression of Ca^{2+} signaling pathway-related genes coupled with a CaSR-MAPK-mediated mechanism to maintain spermatogenesis can explain instances of abnormal meiosis progression in pseudomales. In addition to a better understanding of the regulation of spermatogenesis in general, the results of this study have important implications for two reasons. First, our results provide a basis for investigations of the reproductive capacity of pseudomales, which are being increasingly found in natural populations of various vertebrate species exposed to elevated temperatures. Second, our results may guide the development of a strategy to correct the differences in spermatogenesis in pseudomales to enhance their reproductive capacity in fish farming. This can be achieved by improving the spermatogenic microenvironment (e.g., by adding androgens, increasing the calcium concentration, or adding CaSR agonists).

Materials and methods

Biological samples and the ethical use of animals

Experimental procedures using Chinese tongue sole were approved by the Animal

Care and Use Committee at the Chinese Academy of Fishery Sciences, and all experimental procedures were performed in accordance with the guidelines for the Care and Use of Laboratory Animals at the Chinese Academy of Fishery Sciences. Chinese tongue sole testes were obtained from 11 normal healthy males (2 years old) and 7 pseudomales (2 years old) that were housed at Haiyang High-Tech Experimental Base (Haiyang, China).

Dissociation of testicular cells in male and pseudomale Chinese tongue sole

To obtain a high-quality cell suspension, the preparation time was strictly controlled. First, the testes of Chinese tongue sole were dissected on ice and washed twice with 5 ml of DMEM + 2% NaCl, and other tissues adhered to the testes were removed with tweezers. The testis tissue was cut with a blade to form the tissue homogenate. The tissue homogenate was transferred to the combined enzyme digestion solution (ratio of trypsin to collagenase: 5 to 1). After heating in a 30 °C water bath for 5–10 min, digestion was rapidly terminated with 6–7 mL of DMEM with 2% NaCl. The digested cell suspension was filtered with a 100 μm filter and filtered again with a 40 μm filter. Approximately 7 mL of the filtered cell suspension was added to a 15 mL tube. Centrifugation was performed with a horizontal rotor in a cryogenic centrifuge at 400 × *g* for 5 min. After removing the supernatant, 7 mL of PBS with 2% NaCl (PBS + 2% NaCl) was added, centrifuged at 400 × *g* for 5 min, and washed twice. Finally, 0.05% BSA in PBS + 2% NaCl was added and cells were resuspended. Then, 10 μL of the single cell suspension was mixed with 1 μL of 0.4% dye trypan blue solution to measure the total cell concentration (1000–2000 cells per 1 μL) as well as the ratio of live cells (greater than 80 percent) using a hemocytometer.

scRNA-seq library preparation and sequencing

The scRNA-seq library was constructed immediately after the cell suspension was prepared. The DNBelab C Series Single Cell RNA Library Preparation Kit was used based on droplet microfluidics technology for library construction. Cells were prepared as droplets in which cell lysis and mRNA capture were performed using the DNBelab C4 portable single-cell system (MGI Tech Co., Ltd.) Single-cell microdroplets were recovered by the emulsion breaking recovery system, after which magnetic bead-captured mRNA was synthesized into cDNA and subjected to 16 cycles of PCR for cDNA enrichment. Finally, cDNA products were used to prepare single-stranded DNA libraries by various steps, such as shearing, end repair, ligation, 12 cycles of PCR, denaturation, circularization, and digestion. Then, 10 ng of the digested product was obtained for sequencing using the MGISEQ 2000 platform.

scRNA-seq data processing

The raw data obtained by scRNA-seq using the MGISEQ2000 platform were filtered and demultiplexed using PISA (version 1.10.2) (https://github.com/shiquan/PISA). Reads were aligned to the reference genome from NCBI using STAR (version 2.7.9a) and sorted using sambamba (version 0.7.0). The cell versus gene UMI count matrix was generated using PISA.

Cell clustering and identification of cell types

A clustering analysis of the testis of the Chinese tongue sole dataset was performed using *Seurat* (version 3.2.3) in R, which allows for the selection and filtration of cells on the basis of quality control metrics, data normalization and scaling, and detection of highly variable genes. In preprocessing, for each dataset, we followed the Seurat process (https://satijalab.org/seurat/articles/pbmc3k_tutorial.html) to create a data matrix object. Cells were filtered based on the following criteria: all genes are expressed in at least three cells and cells contain more than 200 detected genes. Then, cells with mitochondrial gene percentages > 5% and unique gene counts < 200 were discarded, and *DoubletFinder* (version 2.0.3) was used to detect doublet cells. Finally, batch correction and integration were performed using the Integrate Data functions in the Seurat package. The merged Seurat objects were scaled and analyzed by principal component analysis (PCA). The first 20 principal components (PCs) were used to construct a KNN graph and refine the edge weights between any two cells. Based on all the local neighborhoods of cells, the *FindClusters* function with the resolution parameter set to 0.5 was used for clustering. Finally, plots were generated using UMAP. The DEGs were identified based on comparisons between each cluster using the *FindAllMarkers* function (test.use = Wilcox) with the logfc.threshold and min.pct parameters set to 0.25.

Fluorescence *in situ* hybridization

To make paraffin sections, the testis tissue was fixed in the fixing agent for at least 24 h. For dehydration and paraffin embedding, samples were placed in 75% ethanol for 4 h, 85% ethanol for 2 h, 90% alcohol for 2 h, 95% ethanol for 1 h, 100% ethanol I for 30 min, 100% ethanol II for 30 min, ethanol benzene for 5–10 min, xylene II for 5–10

min, 65°C melting paraffin I for 1 h, 65°C melting paraffin II for 1 h, and 65°C melting paraffin III for 1 h. The wax-soaked tissue was embedded using an embedding machine. Samples were cooled at -20°C on a freezing table. After the wax solidified, the wax block was removed from the embedding frame and repaired. The trimmed wax block was sectioned on a microtome paraffin slicer with a thickness of 4 μm.

For HE staining, dewaxing was performed by rinsing in xylene I for 20 min, xylene II for 20 min, 100% ethanol I for 5 min, 100% ethanol II for 5 min, and 75% ethanol for 5 min. Sections were then rinsed with tap water, stained with hematoxylin solution for 3–5 min, and rinsed with tap water. Then, the sections were treated with Hematoxylin Differentiation solution and rinsed with tap water. The sections were treated with Hematoxylin Scott Tap Bluing and rinsed with tap water. They were then treated with 85% ethanol for 5 min and 95% ethanol for 5 min. Finally, sections were stained with Eosin dye for 5 min. For dehydration, sections were treated with 100% ethanol I for 5 min, 100% ethanol II for 5 min, 100% ethanol III for 5 min, xylene I for 5 min, and xylene II for 5 min, followed by sealing with neutral gum. Sections were observed by microscopy and images were obtained for analysis.

For fluorescence *in situ* hybridization, the mRNA sequence of the target gene was searched against the NCBI database. The oligonucleotide probe sequence was designed using Primer 5.0 (Primer-E Ltd., Plymouth, UK) The fluorescent probe was synthesized by Sangon Biotech (Shanghai, China). Fluorescence *in situ* hybridization was performed using the RNA-FISH Kit (GenePharma, Shanghai, China).

Functional enrichment analysis

A functional enrichment analysis of DEGs was performed using Metascape (https://metascape.org/gp/index.html) (Zhou et al., 2019). Chinese tongue sole genes used for the enrichment analysis were homologous to zebrafish genes.

Conservation of marker gene expression

Mouse and human UMI matrices were obtained from the NCBI Gene Expression Omnibus (GEO) database (accession numbers GSE112393 and GSE106487). Germ and somatic cells were extracted from two matrices according to the barcode of the cell type reported previously (Green et al., 2018; Wang et al., 2018). Then, we detected marker genes in Chinese tongue sole germ cells and somatic testicular cells, and Z-scores were calculated to draw a heatmap for the comparison of spermatogenesis in these two species and Chinese tongue sole.

Cell trajectory analysis

Single-cell pseudotime trajectories were constructed using Monocle 2 (version 2.14.0) (http://cole-trapnell-lab.github.io/monocle-release/docs/) and Monocle3 (version 0.2.2) (https://cole-trapnell-lab.github.io/monocle3/docs/trajectories/). To describe the process of spermatogenesis, the Seurat dataset was input as the cell dataset in Monocle 2 and the "differentialGeneTest" function was used to identify DEGs in each cluster. Genes with a q-value <0.01 were ordered by the pseudotime analysis. Following the same methods, the UMI count matrices of the pre-Lep and P-SPC & sperm cells were also input as an expression matrix, and meta.data was input as the

673 sample sheet. Then, the ordered genes were chosen to define cell progression.
674 DDRTree was used to reduce the dimensionality, and all cells were ordered using the
675 orderCells function. Monocle3 was used to describe the process of sperm maturation.
676 The ordering genes were calculating using the “graph_test” function and filtered with
677 a morans_I > 0.05.

678

679 **Identification of differentially expressed genes**

680 The Seurat *FindAllMarker*s function was used with default options to predict DEGs
681 by comparing each cluster versus all other clusters (with only.pos equal to TRUE,
682 min.pct and logfc.threshold equal to 0.25 and test.use equal to “wilcox”). However,
683 the numbers of DEGs identified by this function in same cell type between males and
684 pseudomales were very small; accordingly, the DESeq2 (v1.30.1) R package was used
685 to find additional DEGs. The package uses non-normalized counts as an input. Data
686 from each sample were aggregated and the *DESeqDataSetFromMatrix* function was
687 used to construct the count matrix. *DESeq* and the *results* function were used for the
688 differential expression analysis and to generate results tables (setting p-value < 0.05
689 and Fold Change > 2 as thresholds).

690

691 **Sex chromosome related-genes analysis**

692 Genes on Z chromosomes were obtained from the GFF file of the genome on the
693 NCBI website. For each germ and somatic cell type, the ratio of the mean expression
694 of all Z chromosome genes to all genes on chromosome 1 was estimated. Next, we
695 selected genes located in the region of dosage compensation on the Z chromosome

and computed the ratio following the same method. To identify Z-specific genes, we compared all Z chromosome genes with autosomes and W chromosome genes by BLASTN with a cutoff identity of >50%, alignment rate >50%, and e-value ≤ 2e-5. In total, 411 genes were homologous to genes on the W chromosome and autosomes. Then, 567 Z genes without any homologues were defined as Z-specific genes for further analysis.

Ethics approval

This study was performed in line with the principles of the Declaration of Helsinki. Approval was granted by the Animal Care and Use Committee at the Chinese Academy of Fishery Sciences (data: August 25, 2021; No: YSFRI-2021015)

Acknowledgements

This work was supported by the National Key R&D Program of China (2018YFD0900301); the National Nature Science Foundation of China (31722058, 31802275 and 31472269); the AoShan Talents Cultivation Program Supported by Qingdao National Laboratory for Marine Science and Technology (2017ASTCP-ES06); the Taishan Scholar Project Fund of Shandong of China to C.S.; the National Ten-Thousands Talents Special Support Program to C.S.; the Central Public-interest Scientific Institution Basal Research Fund, CAFS (No. 2020TD19); and the China Agriculture Research System (CARS-47-G03).

Author contributions

C.S., F.P. and S.L. designed and supervised the research. X.L., J.-Y.C., M.Y., X.Z., W.M. and L.M. performed all experiments, collected and interpreted the data. Y.H., Y.L., F.T. S.L. K.L. and Q.L. did the bioinformatics analysis of single-cell transcriptomic data. S.L., J.-Y.C., G.F., N.R., Q.W. and Y.Q. provided essential reagents and suggestions. Y.Y., X.L. and H.-Y.W. collected the fish samples. H.-Y.W., X.L., Y.H., Y.L. and J.-Y.C. analyzed the data and wrote the manuscript. H.-Y.W., X.L., J.-Y.C., R.N., C.S. and F.P. edited the manuscript and revised it critically. All authors took part in the interpretation of data.

Conflict of interest

The authors declare that they have no conflict of interest.

Data availability

The data reported in this study are available in the CNGB Nucleotide Sequence Archive (CNSA: https:// db.cngb.org/cnsa; accession number CNP0002135).

References

Abby, E., Tourpin, S., Ribeiro, J., Daniel, K., Messiaen, S., Moison, D., Guerquin, J., Gaillard, J.C., Armengaud, J., Langa, F., Toth, A., Martini, E., and Livera, G. (2016). Implementation of meiosis prophase I programme requires a conserved retinoid-independent stabilizer of meiotic transcripts. Nat Commun 7, 10324.

Abdel-Aziz, E.H., Bawazeer, F.A., El-Sayed Ali, T., and Al-Otaibi, M. (2012). Sexual patterns and protogynous sex reversal in the rusty parrotfish, Scarus ferrugineus (Scaridae): histological and physiological studies. Fish Physiol Biochem 38, 1211-1224.

Agarwal, A., Baskaran, S., Parekh, N., Cho, C.L., Henkel, R., Vij, S., Arafa, M., Panner Selvam, M.K., and Shah, R. (2021). Male infertility. Lancet 397, 319-333.

744 Avner, P., and Heard, E. (2001). X-chromosome inactivation: counting, choice and initiation. Nat Rev
745 Genet 2, 59-67.
746 Baltus, A.E., Menke, D.B., Hu, Y.C., Goodheart, M.L., Carpenter, A.E., de Rooij, D.G., and Page, D.C.
747 (2006). In germ cells of mouse embryonic ovaries, the decision to enter meiosis precedes premeiotic
748 DNA replication. Nat Genet 38, 1430-1434.
749 Bas, L., Papinski, D., Licheva, M., Torggler, R., Rohringer, S., Schuschnig, M., and Kraft, C. (2018).
750 Reconstitution reveals Ykt6 as the autophagosomal SNARE in autophagosome-vacuole fusion. J Cell
751 Biol 217, 3656-3669.
752 Bolcun-Filas, E., Rinaldi, V.D., White, M.E., and Schimenti, J.C. (2014). Reversal of female infertility
753 by Chk2 ablation reveals the oocyte DNA damage checkpoint pathway. Science 343, 533-536.
754 Cao, C., Wen, Y., Wang, X., Fang, N., Yuan, S., and Huang, X. (2018). Testicular piRNA profile
755 comparison between successful and unsuccessful micro-TESE retrieval in NOA patients. J Assist
756 Reprod Genet 35, 801-808.
757 Castelli, M.A., Whiteley, S.L., Georges, A., and Holleley, C.E. (2020). Cellular calcium and redox
758 regulation: the mediator of vertebrate environmental sex determination? Biol Rev Camb Philos Soc 95,
759 680-695.
760 Chen, S., Zhang, G., Shao, C., Huang, Q., Liu, G., Zhang, P., Song, W., An, N., Chalopin, D., Volff,
761 J.N., Hong, Y., Li, Q., Sha, Z., Zhou, H., Xie, M., Yu, Q., Liu, Y., Xiang, H., Wang, N., Wu, K., Yang,
762 C., Zhou, Q., Liao, X., Yang, L., Hu, Q., Zhang, J., Meng, L., Jin, L., Tian, Y., Lian, J., Yang, J., Miao,
763 G., Liu, S., Liang, Z., Yan, F., Li, Y., Sun, B., Zhang, H., Zhang, J., Zhu, Y., Du, M., Zhao, Y., Schartl,
764 M., Tang, Q., and Wang, J. (2014). Whole-genome sequence of a flatfish provides insights into ZW sex
765 chromosome evolution and adaptation to a benthic lifestyle. Nat Genet 46, 253-260.
766 Chiang, H.S., Wu, Y.N., Wu, C.C., and Hwang, J.L. (2013). Cytogenic and molecular analyses of
767 46,XX male syndrome with clinical comparison to other groups with testicular azoospermia of genetic
768 origin. J Formos Med Assoc 112, 72-78.
769 Chiarella, P., Puglisi, R., Sorrentino, V., Boitani, C., and Stefanini, M. (2004). Ryanodine receptors are
770 expressed and functionally active in mouse spermatogenic cells and their inhibition interferes with
771 spermatogonial differentiation. J Cell Sci 117, 4127-4134.
772 Colozza, G., and Koo, B.K. (2021). Ub and Dub of RNF43/ZNRF3 in the WNT signalling pathway.
773 EMBO Rep 22, e52970.
774 Conigrave, A.D., and Ward, D.T. (2013). Calcium-sensing receptor (CaSR): pharmacological properties
775 and signaling pathways. Best Pract Res Clin Endocrinol Metab 27, 315-331.
776 Culty, M., Liu, Y., Manku, G., Chan, W.Y., and Papadopoulos, V. (2015). Expression of
777 steroidogenesis-related genes in murine male germ cells. Steroids 103, 105-114.
778 De Fazio, S., Bartonicek, N., Di Giacomo, M., Abreu-Goodger, C., Sankar, A., Funaya, C., Antony, C.,
779 Moreira, P.N., Enright, A.J., and O'Carroll, D. (2011). The endonuclease activity of Mili fuels piRNA
780 amplification that silences LINE1 elements. Nature 480, 259-263.
781 Endo, T., Romer, K.A., Anderson, E.L., Baltus, A.E., de Rooij, D.G., and Page, D.C. (2015). Periodic
782 retinoic acid-STRA8 signaling intersects with periodic germ-cell competencies to regulate
783 spermatogenesis. Proc Natl Acad Sci U S A 112, E2347-2356.
784 Estermann, M.A., Williams, S., Hirst, C.E., Roly, Z.Y., Serralbo, O., Adhikari, D., Powell, D., Major,
785 A.T., and Smith, C.A. (2020). Insights into Gonadal Sex Differentiation Provided by Single-Cell
786 Transcriptomics in the Chicken Embryo. Cell Rep 31, 107491.

787 Fujihara, Y., Noda, T., Kobayashi, K., Oji, A., Kobayashi, S., Matsumura, T., Larasati, T., Oura, S.,
788 Kojima-Kita, K., Yu, Z., Matzuk, M.M., and Ikawa, M. (2019). Identification of multiple male
789 reproductive tract-specific proteins that regulate sperm migration through the oviduct in mice. Proc
790 Natl Acad Sci U S A 116, 18498-18506.
791 García-López, A., Bogerd, J., Granneman, J.C., van Dijk, W., Trant, J.M., Taranger, G.L., and Schulz,
792 R.W. (2009). Leydig cells express follicle-stimulating hormone receptors in African catfish.
793 Endocrinology 150, 357-365.
794 Green, C.D., Ma, Q., Manske, G.L., Shami, A.N., Zheng, X., Marini, S., Moritz, L., Sultan, C.,
795 Gurczynski, S.J., Moore, B.B., Tallquist, M.D., Li, J.Z., and Hammoud, S.S. (2018). A Comprehensive
796 Roadmap of Murine Spermatogenesis Defined by Single-Cell RNA-Seq. Dev Cell 46, 651-667.e610.
797 Griswold, M.D. (2016). Spermatogenesis: The Commitment to Meiosis. Physiol Rev 96, 1-17.
798 Guan, J., Kinoshita, M., and Li, Y. (2009). Spatiotemporal association of DNAJB13 with the annulus
799 during mouse sperm flagellum development. BMC Developmental Biology 9, 23-23.
800 Guillaume, E., Evrard, B., Com, E., Moertz, E., Jégou, B., and Pineau, C. (2010). Proteome analysis of
801 rat spermatogonia: Reinvestigation of stathmin spatio-temporal expression within the testis. Molecular
802 Reproduction & Development 60.
803 Guioli, S., Lovell-Badge, R., and Turner, J.M. (2012). Error-prone ZW pairing and no evidence for
804 meiotic sex chromosome inactivation in the chicken germ line. PLoS Genet 8, e1002560.
805 Guo, J., Grow, E.J., Mlcochova, H., Maher, G.J., Lindskog, C., Nie, X., Guo, Y., Takei, Y., Yun, J., Cai,
806 L., Kim, R., Carrell, D.T., Goriely, A., Hotaling, J.M., and Cairns, B.R. (2018). The adult human testis
807 transcriptional cell atlas. Cell Res 28, 1141-1157.
808 Guo, J., Grow, E.J., Yi, C., Mlcochova, H., and Cairns, B.R. (2017). Chromatin and single-cell RNA-
809 seq profiling reveal dynamic signaling and metabolic transitions during human spermatogonial stem
810 cell development. Cell stem cell 21, 533-546.e536.
811 He, Z., Jiang, J., Kokkinaki, M., Golestaneh, N., Hofmann, M.C., and Dym, M. (2008). Gdnf
812 upregulates c-Fos transcription via the Ras/Erk1/2 pathway to promote mouse spermatogonial stem cell
813 proliferation. Stem Cells 26, 266-278.
814 Hess, R.A., and Renato de Franca, L. (2008). Spermatogenesis and cycle of the seminiferous
815 epithelium. Adv Exp Med Biol 636, 1-15.
816 Hurley, D.J., Wilson, R.A., Baldwin, C.L., Liu, J.-Y., and Mastro, A.M. (1994). Characterization of
817 resting and phorbol ester or concanavalin A activated bovine lymph node cells with leukocyte specific
818 monoclonal antibodies. Vet Immunol Immunopathol 40, 49-61.
819 Kamaliyan, Z., Pouriamanesh, S., Soosanabadi, M., Gholami, M., and Mirfakhraie, R. (2018).
820 Investigation of piwi-interacting RNA pathway genes role in idiopathic non-obstructive azoospermia.
821 Sci Rep 8, 142.
822 Kazarian, E., Son, H., Sapao, P., Li, W., Zhang, Z., Strauss, J.F., and Teves, M.E. (2018). SPAG17 Is
823 Required for Male Germ Cell Differentiation and Fertility. Int J Mol Sci 19.
824 Krausz, C., and Casamonti, E. (2017). Spermatogenic failure and the Y chromosome. Hum Genet 136,
825 637-655.
826 Kurtz, K., Martínez-Soler, F., Ausió, J., and Chiva, M. (2007). Acetylation of histone H4 in complex
827 structural transitions of spermiogenic chromatin. J Cell Biochem 102, 1432-1441.
828 Kurusu, S., Sapirstein, A., Sawada, H., Kawaminami, M., and Bonventre, J.V. (2011). Group IVA
829 phospholipase A2 regulates testosterone biosynthesis by murine Leydig cells and is required for timely

sexual maturation. Biochem J 439, 403-411.
Lau, X., Munusamy, P., Ng, M.J., and Sangrithi, M. (2020a). Single-Cell RNA Sequencing of the Cynomolgus Macaque Testis Reveals Conserved Transcriptional Profiles during Mammalian Spermatogenesis. Dev Cell 54, 548-566.e547.
Lau, X., Munusamy, P., Ng, M.J., and Sangrithi, M. (2020b). Single-Cell RNA Sequencing of the Cynomolgus Macaque Testis Reveals Conserved Transcriptional Profiles during Mammalian Spermatogenesis. Dev Cell.
Lauper, N., Beck, A.R., Cariou, S., Richman, L., Hofmann, K., Reith, W., Slingerland, J.M., and Amati, B. (1998). Cyclin E2: a novel CDK2 partner in the late G1 and S phases of the mammalian cell cycle. Oncogene 17, 2637.
Law, N.C., Oatley, M.J., and Oatley, J.M. (2019). Developmental kinetics and transcriptome dynamics of stem cell specification in the spermatogenic lineage. Nat Commun 10, 2787.
Leal, M.C., Cardoso, E.R., Nóbrega, R.H., Batlouni, S.R., Bogerd, J., França, L.R., and Schulz, R.W. (2009). Histological and stereological evaluation of zebrafish (Danio rerio) spermatogenesis with an emphasis on spermatogonial generations. Biol Reprod 81, 177-187.
Lee, J., Kanatsu-Shinohara, M., Inoue, K., Ogonuki, N., Miki, H., Toyokuni, S., Kimura, T., Nakano, T., Ogura, A., and Shinohara, T. (2007). Akt mediates self-renewal division of mouse spermatogonial stem cells. Development 134, 1853-1859.
Li, M.W., Mruk, D.D., and Cheng, C.Y. (2009). Mitogen-activated protein kinases in male reproductive function. Trends Mol Med 15, 159-168.
Li, X.Y., Mei, J., Ge, C.T., Liu, X.L., and Gui, J.F. (2022). Sex determination mechanisms and sex control approaches in aquaculture animals. Sci China Life Sci 65, 1091-1122.
Lin, Y., Gill, M.E., Koubova, J., and Page, D.C. (2008). Germ cell-intrinsic and -extrinsic factors govern meiotic initiation in mouse embryos. Science 322, 1685-1687.
Lundholm, M., Mayans, S., Motta, V., Lofgren-Burstrom, A., Danska, J., and Holmberg, D. (2010). Variation in the Cd3 zeta (Cd247) gene correlates with altered T cell activation and is associated with autoimmune diabetes. Journal of Immunology 184, 5537-5544.
McElreavey, K., Jorgensen, A., Eozenou, C., Merel, T., Bignon-Topalovic, J., Tan, D.S., Houzelstein, D., Buonocore, F., Warr, N., Kay, R.G.G., Peycelon, M., Siffroi, J.P., Mazen, I., Achermann, J.C., Shcherbak, Y., Leger, J., Sallai, A., Carel, J.C., Martinerie, L., Le Ru, R., Conway, G.S., Mignot, B., Van Maldergem, L., Bertalan, R., Globa, E., Brauner, R., Jauch, R., Nef, S., Greenfield, A., and Bashamboo, A. (2020). Pathogenic variants in the DEAH-box RNA helicase DHX37 are a frequent cause of 46,XY gonadal dysgenesis and 46,XY testicular regression syndrome. Genet Med 22, 150-159.
McGowan, T.A., Madesh, M., Zhu, Y., Wang, L., Russo, M., Deelman, L., Henning, R., Joseph, S., Hajnoczky, G., and Sharma, K. (2002). TGF-beta-induced Ca(2+) influx involves the type III IP(3) receptor and regulates actin cytoskeleton. Am J Physiol Renal Physiol 282, F910-920.
Meng, L., Zhu, Y., Zhang, N., Liu, W., Liu, Y., Shao, C., Wang, N., and Chen, S. (2014). Cloning and characterization of tesk1, a novel spermatogenesis-related gene, in the tongue sole (Cynoglossus semilaevis). PLoS One 9, e107922.
Ming, X., Zhou, Z., Chao, C., Wei, Z., and Mao, Y. (2001). Cloning and characterization of a novel human TEKTIN1 gene. International Journal of Biochemistry & Cell Biology 33, 1172-1182.
Munday, A.D., Berndt, M.C., and Mitchell, C.A. (2000). Phosphoinositide 3-kinase forms a complex with platelet membrane glycoprotein Ib-IX-V complex and 14-3-3zeta. Blood 96, 577-584.

873 Myla, A., Dasmahapatra, A.K., and Tchounwou, P.B. (2021). Sex-reversal and Histopathological
874 Assessment of Potential Endocrine-Disrupting Effects of Graphene Oxide on Japanese medaka
875 (Oryzias latipes) Larvae. Chemosphere 279, 130768.
876 Narita, S., Kageyama, D., Nomura, M., and Fukatsu, T. (2007). Unexpected mechanism of symbiont-
877 induced reversal of insect sex: feminizing Wolbachia continuously acts on the butterfly Eurema hecabe
878 during larval development. Appl Environ Microbiol 73, 4332-4341.
879 Neesen, J., Koehler, M.R., Kirschner, R., Steinlein, C., Kreutzberger, J., Engel, W., and Schmid, M.
880 (1997). Identification of dynein heavy chain genes expressed in human and mouse testis: chromosomal
881 localization of an axonemal dynein gene. Gene 200, 193-202.
882 Oatley, J.M., Avarbock, M.R., and Brinster, R.L. (2007). Glial cell line-derived neurotrophic factor
883 regulation of genes essential for self-renewal of mouse spermatogonial stem cells is dependent on Src
884 family kinase signaling. J Biol Chem 282, 25842-25851.
885 Ohta, T., Miyake, H., Miura, C., Kamei, H., Aida, K., and Miura, T. (2007). Follicle-stimulating
886 hormone induces spermatogenesis mediated by androgen production in Japanese eel, Anguilla japonica.
887 Biol Reprod 77, 970-977.
888 Pan, L., Liu, Q., Li, J., Wu, W., Wang, X., Zhao, D., and Ma, J. (2017). Association of the VDAC3 gene
889 polymorphism with sperm count in Han-Chinese population with idiopathic male infertility. Oncotarget
890 8, 45242-45248.
891 Piferrer, F., and Anastasiadi, D. (2021). Do the Offspring of Sex Reversals Have Higher Sensitivity to
892 Environmental Perturbations? Sex Dev 15, 134-147.
893 Qiu, C.Z., Wang, M.Z., Yu, W.S., Guo, Y.T., Wang, C.X., and Yang, X.F. (2016). Correlation of
894 GOLPH3 Gene with Wnt Signaling Pathway in Human Colon Cancer Cells. J Cancer 7, 928-934.
895 Quinn, A.E., Georges, A., Sarre, S.D., Guarino, F., Ezaz, T., and Graves, J.A. (2007). Temperature sex
896 reversal implies sex gene dosage in a reptile. Science 316, 411.
897 Raverdeau, M., Gely-Pernot, A., Féret, B., Dennefeld, C., Benoit, G., Davidson, I., Chambon, P., Mark,
898 M., and Ghyselinck, N.B. (2012). Retinoic acid induces Sertoli cell paracrine signals for spermatogonia
899 differentiation but cell autonomously drives spermatocyte meiosis. Proc Natl Acad Sci U S A 109,
900 16582-16587.
901 Schulz, R.W., de França, L.R., Lareyre, J.J., Le Gac, F., Chiarini-Garcia, H., Nobrega, R.H., and Miura,
902 T. (2010). Spermatogenesis in fish. Gen Comp Endocrinol 165, 390-411.
903 Schulz, R.W., Menting, S., Bogerd, J., França, L.R., Vilela, D.A., and Godinho, H.P. (2005). Sertoli cell
904 proliferation in the adult testis--evidence from two fish species belonging to different orders. Biol
905 Reprod 73, 891-898.
906 Segaloff, D.L. (2009). Diseases associated with mutations of the human lutropin receptor. Prog Mol
907 Biol Transl Sci 89, 97-114.
908 Shao, C., Li, Q., Chen, S., Zhang, P., Lian, J., Hu, Q., Sun, B., Jin, L., Liu, S., Wang, Z., Zhao, H., Jin,
909 Z., Liang, Z., Li, Y., Zheng, Q., Zhang, Y., Wang, J., and Zhang, G. (2014). Epigenetic modification
910 and inheritance in sexual reversal of fish. Genome Res 24, 604-615.
911 Spruck, C.H., de Miguel, M.P., Smith, A.P., Ryan, A., Stein, P., Schultz, R.M., Lincoln, A.J., Donovan,
912 P.J., and Reed, S.I. (2003). Requirement of Cks2 for the first metaphase/anaphase transition of
913 mammalian meiosis. Science 300, 647-650.
914 Stelkens, R.B., and Wedekind, C. (2010). Environmental sex reversal, Trojan sex genes, and sex ratio
915 adjustment: conditions and population consequences. Mol Ecol 19, 627-646.

916 Tsang, J.C.H., Vong, J.S.L., Ji, L., Poon, L.C.Y., Jiang, P., Lui, K.O., Ni, Y.B., To, K.F., Cheng, Y.K.Y.,
917 Chiu, R.W.K., and Lo, Y.M.D. (2017). Integrative single-cell and cell-free plasma RNA transcriptomics
918 elucidates placental cellular dynamics. Proc Natl Acad Sci U S A 114, E7786-e7795.
919 Valdivieso, A., Wilson, C.A., Amores, A., da Silva Rodrigues, M., Nóbrega, R.H., Ribas, L.,
920 Postlethwait, J.H., and Piferrer, F. (2022). Environmentally-induced sex reversal in fish with
921 chromosomal vs. polygenic sex determination. Environ Res 213, 113549.
922 Wang, M., Liu, X., Chang, G., Chen, Y., An, G., Yan, L., Gao, S., Xu, Y., Cui, Y., Dong, J., Chen, Y.,
923 Fan, X., Hu, Y., Song, K., Zhu, X., Gao, Y., Yao, Z., Bian, S., Hou, Y., Lu, J., Wang, R., Fan, Y., Lian,
924 Y., Tang, W., Wang, Y., Liu, J., Zhao, L., Wang, L., Liu, Z., Yuan, R., Shi, Y., Hu, B., Ren, X., Tang, F.,
925 Zhao, X.Y., and Qiao, J. (2018). Single-Cell RNA Sequencing Analysis Reveals Sequential Cell Fate
926 Transition during Human Spermatogenesis. Cell stem cell 23, 599-614.e594.
927 Wang, Y., Medvid, R., Melton, C., Jaenisch, R., and Blelloch, R. (2007). DGCR8 is essential for
928 microRNA biogenesis and silencing of embryonic stem cell self-renewal. Nat Genet 39, 380-385.
929 Wang, Z., Pan, Y., He, L., Song, X., and Lan, X. (2020). Multiple morphological abnormalities of the
930 sperm flagella (MMAF)-associated genes: The relationships between genetic variation and litter size in
931 goats. Gene 753, 144778.
932 Warr, N., Siggers, P., Bogani, D., Brixey, R., Pastorelli, L., Yates, L., Dean, C.H., Wells, S., Satoh, W.,
933 Shimono, A., and Greenfield, A. (2009). Sfrp1 and Sfrp2 are required for normal male sexual
934 development in mice. Dev Biol 326, 273-284.
935 Watanabe, T., and Lin, H. (2014). Posttranscriptional regulation of gene expression by Piwi proteins
936 and piRNAs. Mol Cell 56, 18-27.
937 Weber, C., Zhou, Y., Lee, J.G., Looger, L.L., Qian, G., Ge, C., and Capel, B. (2020). Temperature-
938 dependent sex determination is mediated by pSTAT3 repression of Kdm6b. Science 368, 303-306.
939 Wu, P.Y., and Nurse, P. (2014). Replication origin selection regulates the distribution of meiotic
940 recombination. Mol Cell 53, 655-662.
941 Xiong, Y., Wang, S., Gui, J.F., and Mei, J. (2020). Artificially induced sex-reversal leads to transition
942 from genetic to temperature-dependent sex determination in fish species. Sci China Life Sci 63, 157-
943 159.
944 Yamaji, M., Jishage, M., Meyer, C., Suryawanshi, H., Der, E., Yamaji, M., Garzia, A., Morozov, P.,
945 Manickavel, S., and Mcfarland, H.L. (2017). DND1 maintains germline stem cells via recruitment of
946 the CCR4–NOT complex to target mRNAs. Nature 543, 568-572.
947 Young, M.D., Mitchell, T.J., Vieira Braga, F.A., Tran, M.G.B., Stewart, B.J., Ferdinand, J.R., Collord,
948 G., Botting, R.A., Popescu, D.M., Loudon, K.W., Vento-Tormo, R., Stephenson, E., Cagan, A., Farndon,
949 S.J., Del Castillo Velasco-Herrera, M., Guzzo, C., Richoz, N., Mamanova, L., Aho, T., Armitage, J.N.,
950 Riddick, A.C.P., Mushtaq, I., Farrell, S., Rampling, D., Nicholson, J., Filby, A., Burge, J., Lisgo, S.,
951 Maxwell, P.H., Lindsay, S., Warren, A.Y., Stewart, G.D., Sebire, N., Coleman, N., Haniffa, M.,
952 Teichmann, S.A., Clatworthy, M., and Behjati, S. (2018). Single-cell transcriptomes from human
953 kidneys reveal the cellular identity of renal tumors. Science 361, 594-599.
954 Zhang, C., Li, Q., Zhu, L., He, W., Yang, C., Zhang, H., Sun, Y., Zhou, L., Sun, Y., Zhu, S., Wu, C., Tao,
955 M., Zhou, Y., Zhao, R., Tang, C., and Liu, S. (2021). Abnormal meiosis in fertile and sterile triploid
956 cyprinid fish. Sci China Life Sci 64, 1917-1928.
957 Zhang, L., Shang, X.J., Li, H.F., Shi, Y.Q., Li, W., Teves, M.E., Wang, Z.Q., Jiang, G.F., Song, S.Z.,
958 and Zhang, Z.B. (2015). Characterization of membrane occupation and recognition nexus repeat

containing 3, meiosis expressed gene 1 binding partner, in mouse male germ cells. Asian J Androl 17, 86-93.
Zhao, L., Yao, C., Xing, X., Jing, T., Li, P., Zhu, Z., Yang, C., Zhai, J., Tian, R., Chen, H., Luo, J., Liu, N., Deng, Z., Lin, X., Li, N., Fang, J., Sun, J., Wang, C., Zhou, Z., and Li, Z. (2020). Single-cell analysis of developing and azoospermia human testicles reveals central role of Sertoli cells. Nat Commun 11, 5683.
Zhou, Y., Zhou, B., Pache, L., Chang, M., Khodabakhshi, A.H., Tanaseichuk, O., Benner, C., and Chanda, S.K. (2019). Metascape provides a biologist-oriented resource for the analysis of systems-level datasets. Nat Commun 10, 1523.
Zirkin, B.R., and Papadopoulos, V. (2018). Leydig cells: formation, function, and regulation. Biol Reprod 99, 101-111.

Figure legends

Figure 1 Overview of germ and somatic testicular cell types determined by scRNA sequencing in Chinese tongue sole. A Schematic showing single-cell RNA-seq of Chinese tongue sole testicular cells. **B** H&E staining of testis sections from male (left) and pseudomale (right) Chinese tongue sole. Scale bars represent 500 μm (top), 200 μm (left lower), and 50 μm (right lower). **C** Visualization of major testis cell types for 31739 cells in UMAP (Unknown is undefined); different cell types are shown in distinct colors, and the number of cells is marked in parentheses. **D** Heatmap showing the expression of the top 20 DEGs for the main cell types. Z-scores were calculated by subtracting the average value for the set of data from the value for each cell and dividing by the standard deviation. **E** Enriched terms for DEGs are shown for germ cell types (*p*-values are shown). **F** Violin plots of the normalized expression of marker genes for the 12 major cell types. **G** Fluorescence *in situ* hybridization for the Undiff SPG marker *gfra1* (green) and spermatocyte marker *ccnb1* (green) in the male testis. Nuclei were visualized using DAPI (blue). Scale bars represent 10 μm (*gfrα1*) and 20 μm (*ccnb1*). **H** Heatmaps of spermatogenic marker gene expression in human, mouse, and Chinese tongue sole. In human, SPG, L, Z, P, D, SPC7, S, and ST

represent spermatogonia, leptotene spermatocytes, zygotene spermatocytes, pachytene spermatocytes, diplotene spermatocytes, secondary spermatocytes, spermatids, and Sertoli cells, respectively. In mouse, SPG, Scytes, STids, and Elongating represent spermatogonia, spermatocytes, round spermatids, and elongating spermatids, respectively.

Figure 2 Germ cell development follows a contiguous trajectory. A Model of spermatogenesis in Chinese tongue sole. Colors represent distinct cell types. The direction of the arrow describes the differentiation process of five germ cell types (from Additional file 1: Figure S3A, B). **B** Gene expression heatmap in pseudotime. After a clustering analysis, genes were divided into four groups (Group A–D). "n" corresponds to the number of genes in each group. **C** Line chart showing the expression trends for marker genes during spermatogenesis (Additional file 1: Figure S3A). **D** UMAP of sperm re-clustering. S1–S4 represent different sperm subclusters: S1 is initial spermatids, S2 is intermediate spermatids, S3 is final spermatids, and S4 is spermatozoa. **E** Heatmap of top20 DEGs at different stages of sperm maturation. Representative markers are listed. **F** Violin plots of the normalized expression of marker genes for the Sperm subclusters. **G** Pseudotime trajectory of sperm maturation.

Figure 3 Integrated analysis of spermatogenesis in male (ZZm) and pseudomale (ZWm) Chinese tongue sole. A Proportion of germ cells in males (blue) and pseudomales (red). Line chart shows the trends in relative frequencies. $p < 0.05$ (*), $p < 0.01$ (**), $p < 0.001$ (***), $p < 0.0001$(****), and "ns" indicates "not significant", determined by *t*-tests. **B** Heatmap and enrichment analysis of all DEGs ($p < 0.05$,

|Log2FC| > 2) in testicular cells from males and pseudomales. The color bar in the header represents males (blue) and pseudomales (red). The color bar at the bottom represents the cell types corresponding to males and pseudomales. **C** Heatmap of cell cycle-specific genes from male (blue) and pseudomale (red) testicular cells. The *y*-axis shows G1/S (top) and G2/M(bottom) phase genes. **D** Box plot showing the expression of meiosis-related genes in germ cells. Gene expression was compared between males and pseudomales. **E** Box plot showing the up-regulated genes in Diff.ed SPG and pre-Lep from pseudomale.

Figure 4 Transcriptional differences in Undiff SPG between males (ZZm) and pseudomales (ZWm). A Volcano plot showing DEGs between spermatogonia from males and pseudomales, setting Fold Change > 2 as the threshold (dotted line). Up-regulated genes in pseudomales are labeled in red, and down-regulated genes are labeled in blue. **B** Enriched terms for DEGs between pseudomale and male Undiff SPG. Red shows pathway enrichment for up-regulated genes in Undiff SPG in pseudomales, and blue shows pathway enrichment for down-regulated genes in Undiff SPG in pseudomales. **C** Heatmap showing the expression of MAPK signaling pathway-related genes in male and pseudomale testicular cells. **D** Differential expression of multiple copies of *CaSR* in Chinese tongue sole Undiff SPG between males and pseudomales. Location information for different copies is indicated on the right. **E** Heatmap showing the expression of Ca^{2+} signaling pathway-related genes in male and pseudomale testicular cells. **F** Box plot showing the expression of *gfrα*1 and *ret* in Undiff SPG of males and pseudomales. $p < 0.05$ (*), $p < 0.001$ (***), determined by *t*-tests.

Figure 5 Z chromosomal gene activity in male (ZZm) and pseudomale (ZWm) Chinese tongue sole testis cells. A Heatmap of the expression of Z chromosome-specific genes (Top) and autosomal genes (bottom) in male and pseudomale testicular cells and an enrichment analysis of Z chromosome-specific genes ($p < 0.05$). **B** Heatmap of piRNA-related gene expression in males and pseudomales. **C** Box plots of Z chromosome-specific genes associated with spermatogenesis in germ cells. $p < 0.05$ (*), $p < 0.01$ (**), $p < 0.001$ (***), $p < 0.0001$ (****), and "ns" indicates "not significant", determined by *t*-tests. **D** Box plot of Z chromosome gene expression in males and pseudomales fish. Z-to-autosome expression ratio indicates the ratio of the average expression of Z chromosome genes to the average expression of autosomal genes. **E** Box plot of dosage-compensation region genes (13.6–15.6 Mb) (Shao et al., 2014) on the Z chromosome in male and pseudomale fish. The Z (13.6–15.6 Mb) to autosome expression ratio indicates the ratio of the average expression of genes in the dosage-compensation region to the average expression of autosomal genes

Figure 6 Transcription profile differences between somatic testicular niche cells of male (ZZm) and pseudomale (ZWm) gonads. A Proportions of somatic cells in males (blue) and pseudomales (red). $p < 0.05$ (*), $p < 0.01$ (**), $p < 0.001$ (***), $p < 0.0001$ (****), and "ns" indicates "not significant", determined by *t*-tests. **B** Volcano plot showing the DEGs in Leydig cells between males and pseudomales, Fold Change > 2 as the threshold (dotted line). **C** Enriched terms for DEGs between male and pseudomale Leydig cells. **D** Heatmap of steroidogenesis-related genes in male and pseudomale fish testis cells. **E** Volcano plot showing the DEGs in Sertoli cells

between males and pseudomales, Fold Change > 2 as the threshold (dotted line). **F** Enriched terms of DEGs between male and pseudomale Sertoli cells. **G** Box plot of down-regulated genes in Sertoli cells of pseudomale. $p < 0.05$ (*), $p < 0.01$ (**), $p < 0.001$ (***), $p < 0.0001$ (****), determined by *t*-tests. **H** Heatmap of sex-related genes in testicular cells of Chinese tongue sole males and pseudomales.

Figure 7 Model of pseudomale spermatogenesis. Pseudomales showed a decrease in the area occupied by Leydig cells, and the down-regulation of several genes related to Leydig and Sertoli cell function. In spermatogonia, the CaSR-MAPK signaling factors *gfrα1* and *ret* are active and Ca2+ signaling is inactive. The meiotic initiation of spermatocytes is blocked, accompanied by autophagy. Many genes related to spermatogenesis are expressed on the Z chromosome; however, they are absent on the W chromosome.

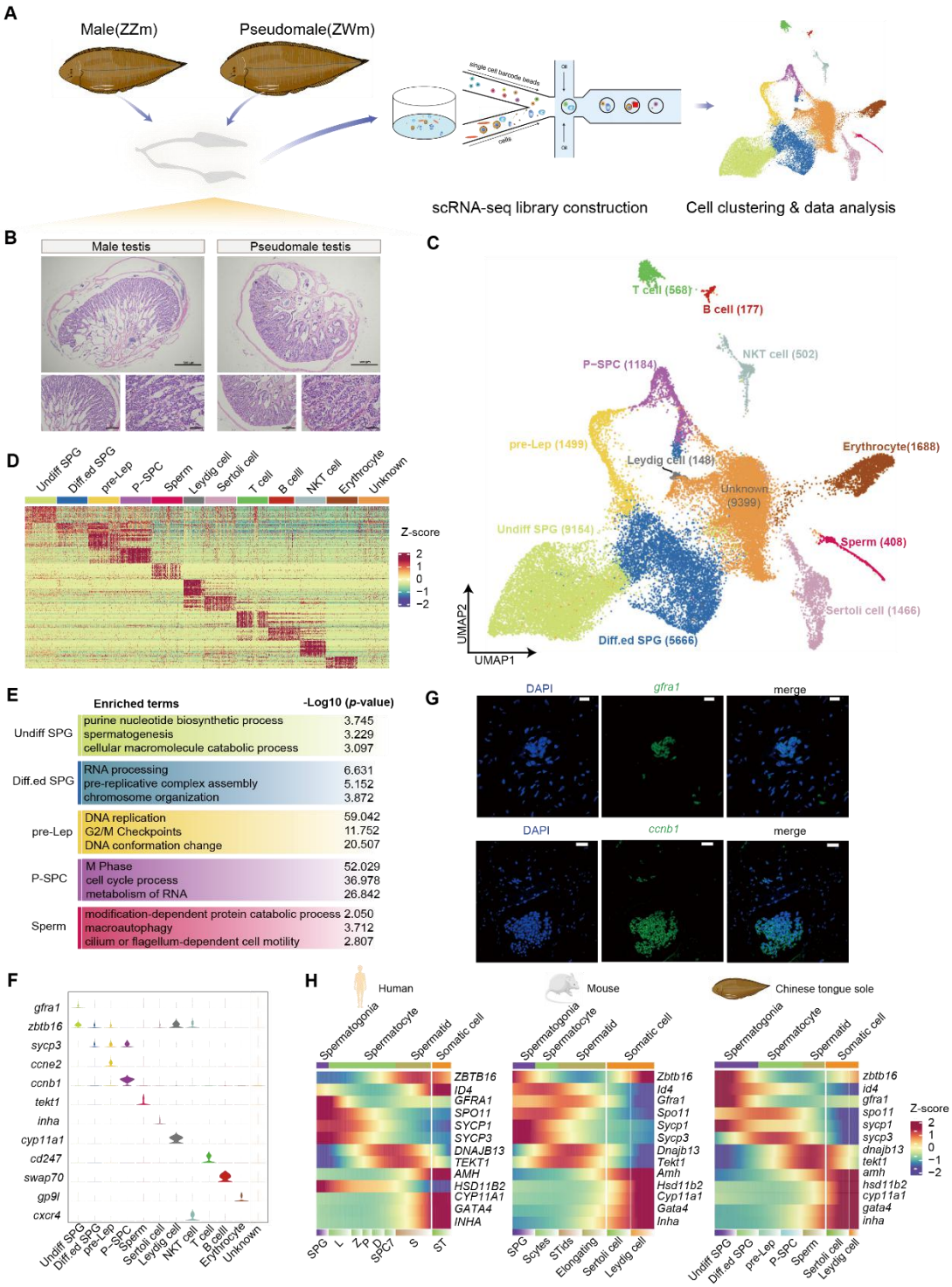

Figure 1 Overview of germ and somatic testicular cell types determined by scRNA sequencing in Chinese tongue sole. A, Schematic showing single-cell RNA-seq of Chinese tongue sole testicular cells. B, H&E staining of testis sections from male (left) and pseudomale (right) Chinese tongue sole. Scale bars represent 500 μm (top), 200 μm (left lower), and 50 μm (right lower). C, Visualization of major testis cell types for 31,739 cells in UMAP (Unknown is undefined),

different cell types are shown in distinct colors, and the number of cells is marked in parentheses. D, Heatmap showing the expression of the top 20 DEGs for the main cell types. Z-scores were calculated by subtracting the average value for the set of data from the value for each cell and dividing by the standard deviation. E, Enriched terms for DEGs are shown for germ cell types (*P*-values are shown). F, Violin plots of the normalized expression of marker genes for the 11 major cell types. G, Fluorescence *in situ* hybridization for the Undiff SPG marker *gfra1* (green) and spermatocyte marker *ccnb1* (green) in the male testis. Nuclei were visualized using DAPI (blue). Scale bars represent 10 μm (*gfrα1*) and 20 μm (*ccnb1*). H, Heatmaps of spermatogenic marker gene expression in human, mouse, and Chinese tongue sole. In human, SPG, L, Z, P, D, SPC7, S, and ST represent spermatogonia, leptotene spermatocytes, zygotene spermatocytes, pachytene spermatocytes, diplotene spermatocytes, secondary spermatocytes, spermatids, and Sertoli cells, respectively. In mouse, SPG, Scytes, STids, and Elongating represent spermatogonia, spermatocytes, round spermatids, and elongating spermatids, respectively.

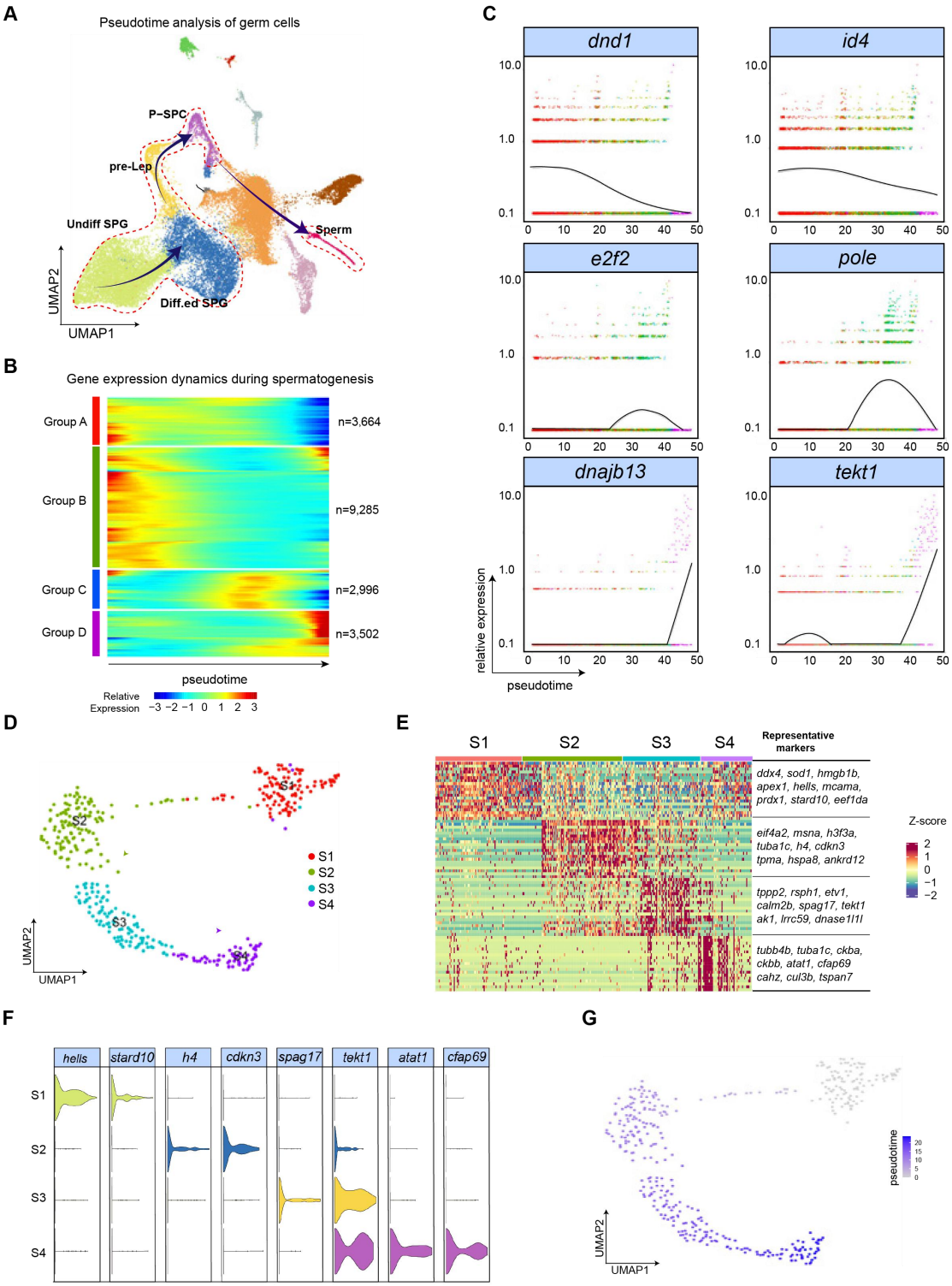

Figure 2 Germ cell development follows a contiguous trajectory. A, Model of spermatogenesis in Chinese tongue sole. Colors represent distinct cell types. The direction of the arrow describes the differentiation process of five germ cell types (from Figure S3A, B in Supporting Information). B, Gene expression heatmap in pseudotime. After a clustering analysis, genes were divided into four groups (Group A–D). "*n*" corresponds to the number of genes in each group. C, Line chart showing the expression trends for marker genes during spermatogenesis (from Figure S3A in Supporting Information). D, UMAP of sperm reclustering. S1–S4 represent different sperm

subclusters: S1 is initial spermatids, S2 is intermediate spermatids, S3 is final spermatids, and S4 is spermatozoa. E, Heatmap of top20 DEGs at different stages of sperm maturation. Representative markers are listed. F, Violin plots of the normalized expression of marker genes for the sperm subclusters. G, Pseudotime trajectory of sperm maturation.

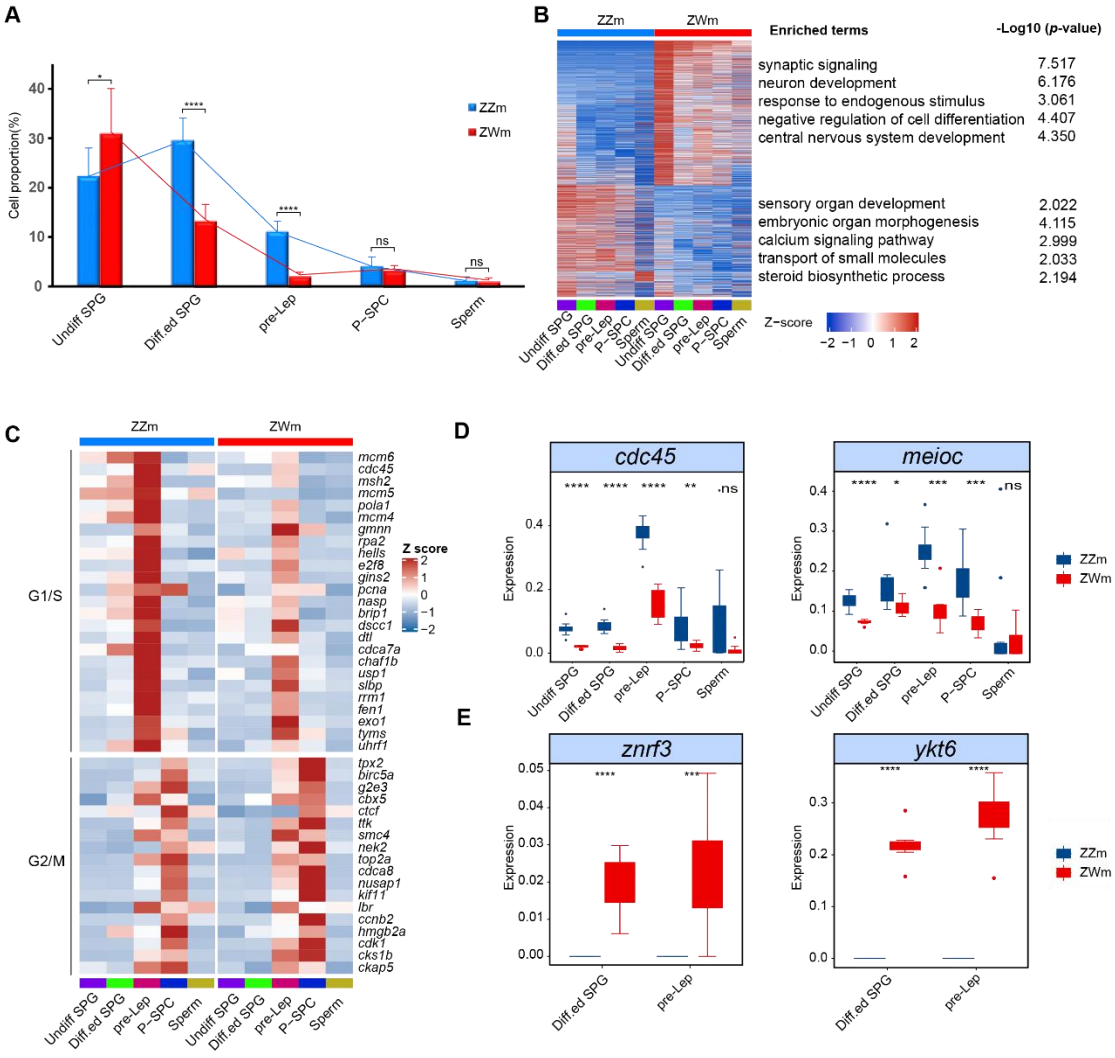

Figure 3 Integrated analysis of spermatogenesis in male (ZZm) and pseudomale (ZWm) Chinese tongue sole. A, Proportion of germ cells in males (blue) and pseudomales (red). Line chart shows the trends in relative frequencies. $P<0.05$ (*), $P<0.01$ (**), $P<0.001$ (***), $P<0.0001$(****), and "ns" indicates "not significant", determined by *t*-tests. B, Heatmap and enrichment analysis of all DEGs ($P<0.05$, |Log2FC|>2) in testicular cells from males and pseudomales. The color bar in the header represents males (blue) and pseudomales (red). The color bar at the bottom represents the cell types corresponding to males and pseudomales. C, Heatmap of cell cycle-specific genes from male (blue) and pseudomale (red) testicular cells. The *y*-axis shows G1/S (top) and G2/M (bottom) phase genes. D, Box plot showing the expression of meiosis-related genes in germ cells. Gene expression was compared between males and pseudomales. E, Box plot showing the up-regulated autophagy genes in Diff.ed SPG and pre-Lep from pseudomale.

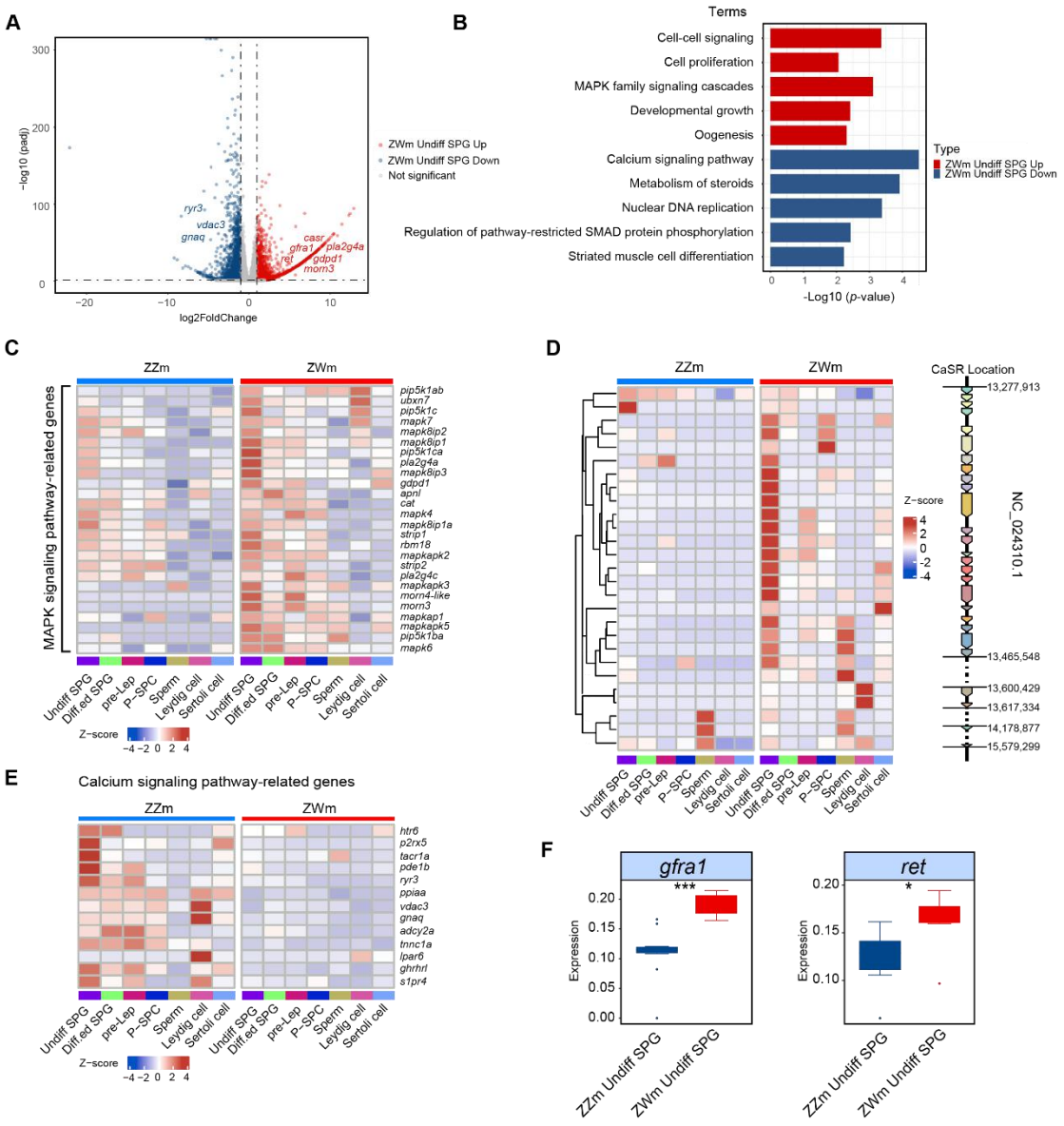

Figure 4 Transcriptional differences in Undiff SPG between males (ZZm) and pseudomales (ZWm). A, Volcano plot showing DEGs between Undiff SPG from males and pseudomales, setting Fold Change >2 as the threshold (dotted line). Up-regulated genes in pseudomales are labeled in red, and downregulated genes are labeled in blue. B, Enriched terms for DEGs between pseudomale and male Undiff SPG. Red shows pathway enrichment for up-regulated genes in Undiff SPG in pseudomales, and blue shows pathway enrichment for down-regulated genes in Undiff SPG in pseudomales. C, Heatmap showing the expression of MAPK signaling pathway-related genes in male and pseudomale testicular cells. D, Differential expression of multiple copies of *CaSR* in Chinese tongue sole Undiff SPG between males and pseudomales. Location information for different copies is indicated on the right. E, Heatmap showing the expression of Ca^{2+} signaling pathway-related genes in male and pseudomale testicular cells. F, Box plot showing the expression of *gfrα*1 and *ret* in Undiff SPG of males and pseudomales. $P<0.05$ (*), $P<0.001$ (***), determined by *t*-tests.

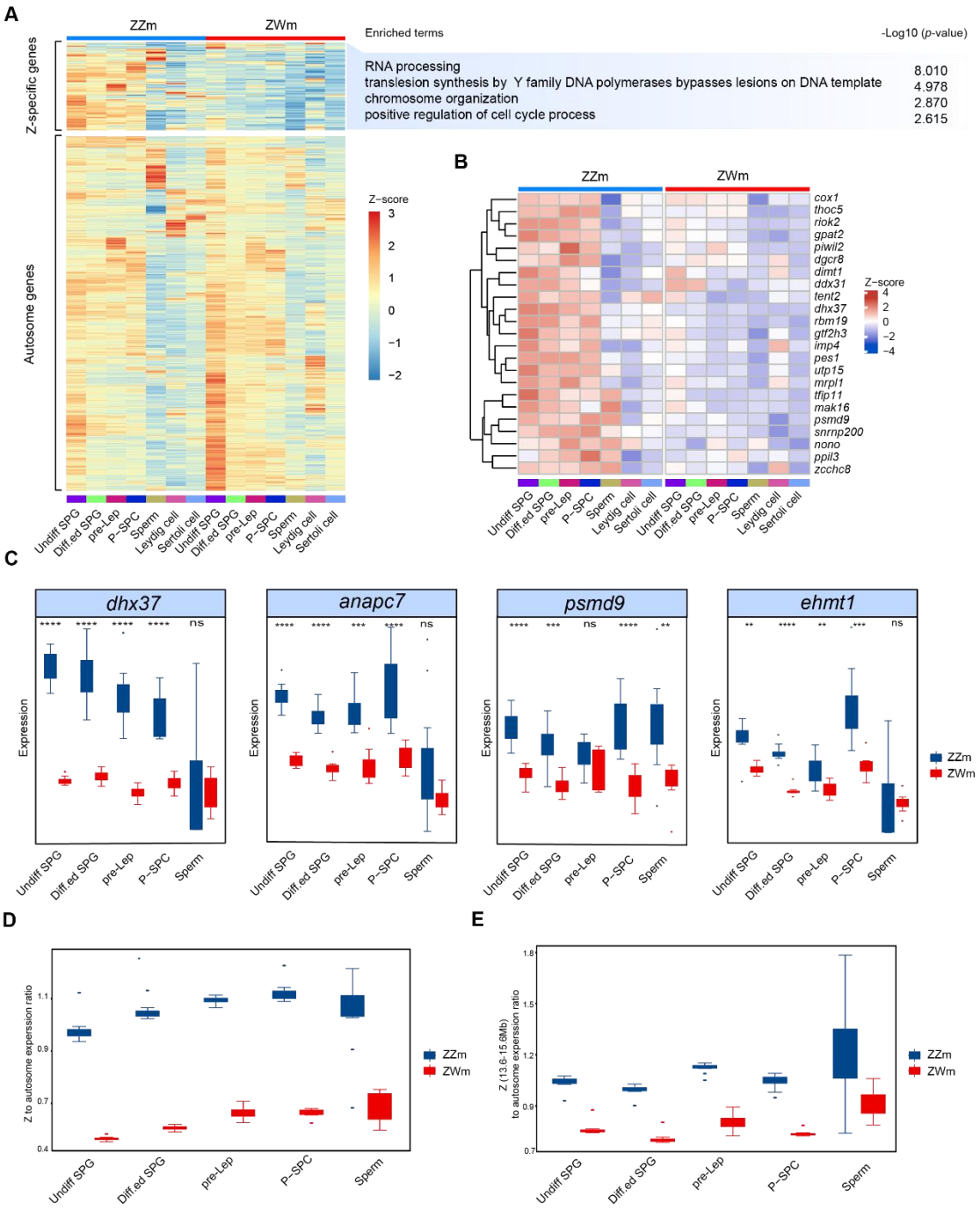

Figure 5 Z chromosomal gene activity in male (ZZm) and pseudomale (ZWm) Chinese tongue sole testis cells. A, Heatmap of the expression of Z chromosome-specific genes (top) and autosomal genes (bottom) in male and pseudomale testicular cells and an enrichment analysis of Z chromosomespecific genes (P<0.05). B, Heatmap of piRNA-related gene expression in males and pseudomales. C, Box plots of Z chromosome-specific genes associated with spermatogenesis in germ cells. P<0.05 (*), P<0.01 (**), P<0.001 (***), P<0.0001 (****), and "ns" indicates "not significant", determined by *t*-tests. D, Box plot of Z chromosome gene expression in males and pseudomales fish. Z-to-autosome expression ratio indicates the ratio of the average expression of Z chromosome genes to the average expression of autosomal genes. E, Box plot of dosage-compensation region genes (13.6–15.6 Mb) (Shao et al., 2014) on the Z chromosome in male and

pseudomale fish. The Z (13.6–15.6 Mb) to autosome expression ratio indicates the ratio of the average expression of genes in the dosage-compensation region to the average expression of autosomal genes.

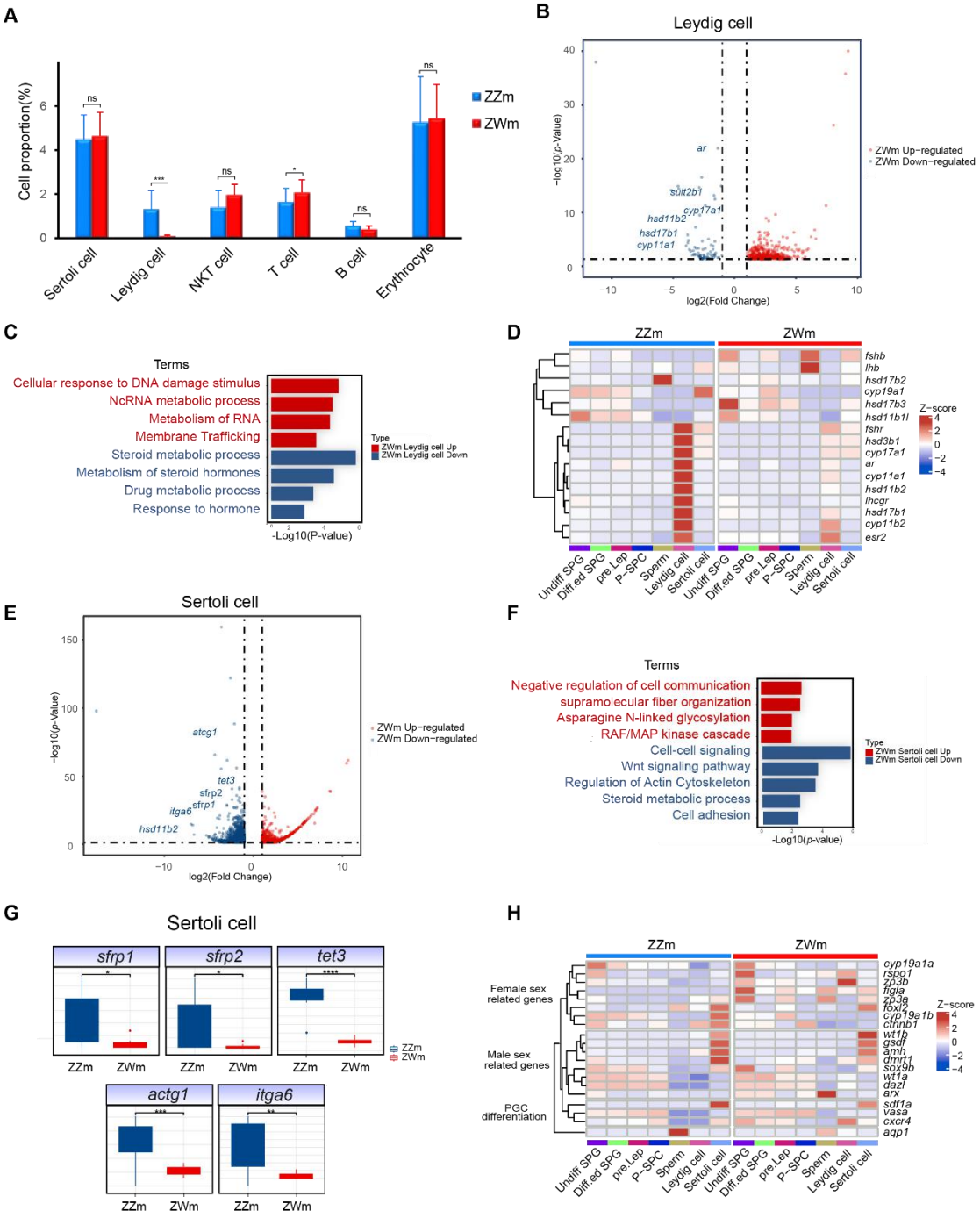

Figure 6 Transcription profile differences between somatic testicular niche cells of male (ZZm) and pseudomale (ZWm) gonads. A, Proportions of somatic cells in males (blue) and pseudomales (red). $P<0.05$ (*), $P<0.01$ (**), $P<0.001$ (***), $P<0.0001$ (****), and "ns" indicates "not significant", determined by *t*-tests. B, Volcano plot showing the DEGs in Leydig cells between males and pseudomales, Fold Change >2 as the threshold (dotted line). C, Enriched terms for DEGs between male and pseudomale Leydig cells. D, Heatmap of steroidogenesis-related genes in

male and pseudomale fish testis cells. E, Volcano plot showing the DEGs in Sertoli cells between males and pseudomales, Fold Change >2 as the threshold (dotted line). F, Enriched terms of DEGs between male and pseudomale Sertoli cells. G, Box plot of down-regulated genes in Sertoli cells of pseudomale. $P<0.05$ (*), $P<0.01$ (**), $P<0.001$ (***), $P<0.0001$ (****), determined by *t*-tests. H, Heatmap of sex-related genes in testicular cells of Chinese tongue sole males and pseudomales.

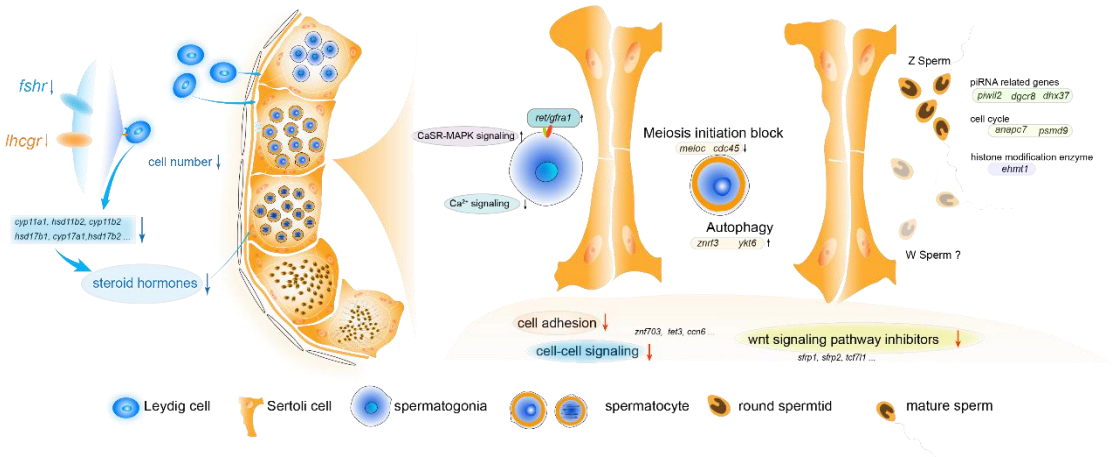

Figure 7 Model of pseudomale spermatogenesis. Pseudomales showed a decrease in the area occupied by Leydig cells, and the down-regulation of several genes related to Leydig and Sertoli cell function. In spermatogonia, the CaSR-MAPK signaling factors *gfrα1* and *ret* are active and Ca^{2+} signaling is inactive. The meiotic initiation of spermatocytes is blocked, accompanied by autophagy. Many genes related to spermatogenesis are expressed on the Z chromosome; however, they are absent on the W chromosome.